Journal of Materials Chemistry A

ROYAL SOCIETY OF CHEMISTRY

REVIEW

View Article Online
View Journal

Cite this: DOI: 10.1039/d6ta02244h

Capacitive deionization for targeted anion removal: mechanisms, advances, and future directions

Yuting Shi,[a] Haoran Xu,[a] Jintian Jiang,[c] Guoqing Xu,[a] Zhiyang Yu,[a] Wei Zhang,[c] Shi Jia,*[b] Ao Yu *[b] and Minjie Shi *[a]

The escalating prevalence of anionic contaminants in water sources presents a critical challenge to global water security. Conventional treatment methods are frequently limited by secondary pollution, high energy consumption, and suboptimal efficacy in complex aqueous matrices. Capacitive deionization (CDI), an emerging electrochemical desalination technology, offers a compelling alternative for selective anion removal, distinguished by its low energy footprint, environmental compatibility, operational simplicity, and designable electrode architectures. This review provides a systematic overview of recent progress in CDI for the removal of key anions, including fluoride, chloride, phosphate, sulfate, and arsenate. It elucidates the fundamental mechanisms underlying ion removal, tracing the evolution from classical electric double layer adsorption toward multi-mechanistic systems that synergistically integrate redox reactions, ion exchange, and surface complexation. The structural characteristics and comparative advantages of various CDI configurations are critically assessed. Furthermore, this review highlights key innovations in functional electrodes and discuss their role in achieving anion-specific selectivity. Despite substantial progress, persistent challenges remain, including material costs, unresolved microscopic adsorption dynamics, and limited industrial scalability. Finally, prospective research directions are outlined, aimed at material multifunctionalization, system intelligence, and application diversification, offering a roadmap for translating CDI from laboratory innovation to practical water treatment solutions.

Received 15th March 2026
Accepted 21st April 2026

DOI: 10.1039/d6ta02244h

rsc.li/materials-a

1. Introduction

Anionic pollution poses a serious threat to global water security, making its effective prevention, control, and removal strategically important for several critical reasons. From an environmental perspective, elevated anion concentrations degrade aquatic habitats and disrupt ecological balance.[1] For instance, fluoride-rich wastewater from semiconductor manufacturing can infiltrate groundwater, degrading habitats for benthic organisms (*e.g.*, small fish and aquatic insects)[2,3] and thus posing a major barrier to pollution control and ecological restoration.[4] Economically, efficient anion removal is essential for producing the high-purity water required by industries like electronics and pharmaceuticals.[5] Even trace Cl^- can corrode metallic components in chips, leading to product failure and significant financial loss.[6] Moreover, advanced removal technologies can significantly reduce the energy consumption and operational costs of industrial wastewater treatment; for example, they have been reported to reduce treatment costs for textile wastewater by 30–40% compared to conventional methods, promoting greener, lower-carbon industrial practices. Socially, excessive anions in drinking water are linked to public health issues, including skeletal fluorosis and dental fluorosis.[7–9] Therefore, effective anion removal is directly tied to the safety of drinking water and public health, representing a critical public health concern with profound social implications.[10] To address this problem, conventional separation methods such as ion exchange (IX), electrodialysis (ED), and reverse osmosis (RO) have been widely

[a]School of Materials Science and Engineering, Jiangsu University of Science and Technology, Zhenjiang, 212003, China. E-mail: shiminjie@just.edu.cn
[b]Nanoscience of Technology Center, University of Central Florida, Orlando, FL 32826, USA. E-mail: Jia.Shi2@ucf.edu; ao.yu@ucf.edu
[c]Zhejiang Research Institute of Chemical Industry Co., Ltd, Hangzhou, 310023, China

Ao Yu

Ao Yu completed his PhD degree at Huazhong University Science and Technology. He joined Prof. Yang's group as a postdoctoral researcher supported by the Preeminent Postdoctoral Program(P3) in Feb. 2023. His research interestsfocus on electrochemical energy storage and conversion.

employed. However, these techniques are associated with significant drawbacks.[11,12] For instance, IX often generates chemical sludge, leading to secondary pollution.[13] ED suffers from high energy consumption due to membrane resistance and water electrolysis, whereas RO is hampered by low water recovery rates and limited selectivity toward specific anions.[14] Consequently, these conventional methods are often challenged in meeting the growing demand for efficient and environmentally benign treatment of complex water sources.[15]

Capacitive deionization (CDI), an emerging electrochemical water treatment technology, demonstrates considerable potential for selective anion removal.[16] Its core advantages include low energy consumption, environmental friendliness, operational simplicity, and highly reusable electrodes. CDI operates by applying an electric field to drive the adsorption of anions onto electrode surfaces or to induce faradaic reactions, thereby effectively separating them from water.[17,18] The trajectory of CDI development can be divided into three distinct phases (Fig. 1). The first phase (1980s–2000s) focused on the theoretical foundations of electric double-layer formation and carbon electrode optimization. The second phase (2010s) introduced membrane-based configurations, especially membrane capacitive deionization (MCDI), which enhancing ion selectivity and energy efficiency. The most recent phase (2020s) has seen the rise of hybrid (HCDI) and flow-electrode (FCDI) architectures, driven by advances in nanomaterials and scalable manufacturing. This review summarizes recent progress in CDI for anion removal, emphasizing electrode design, desorption mechanisms, and practical application potential, aiming to provide insights for further development and industrialization.[19,20]

2. Overview of CDI technology

2.1. Fundamental principles

CDI technology utilizes electrochemical processes at electrode materials to selectively remove trace harmful anions, such as F- from semiconductor wastewater, Cl^- from textile effluent, and PO_4^{3-} from agricultural runoff.[21,22] The process involves applying a low external voltage (typically 0.4–1.6 V), which attracts target anions to oppositely charged electrodes where they are immobilized *via* electrosorptive or other specific interactions, thereby separating them from the water. This technology offers significant advantages, including low energy consumption, high water recovery rates, and electrode reusability. These combined attributes make it a key emerging technology for the removal of trace harmful anions from water (Fig. 2). The underlying principle of CDI is relatively simple.[16,18,23] When a low voltage is applied between a pair of porous electrodes, ions in the aqueous solution migrate towards the electrode of opposite charge, enabling the selective capture and subsequent removal of target ions.[23–25] For instance, F^- in groundwater can be electrostatically drawn to and retained on the positively charged electrode. This process can effectively reduce fluoride concentration from an initial level of 5 mg L^{-1} to below the World Health Organization (WHO) drinking water guideline of 1.5 mg L^{-1}.[26,27]

Ion removal in CDI proceeds through multiple mechanisms.[28–30] The primary mechanism in conventional CDI is electrosorption *via* the formation of an electric double layer (EDL), a thin ionic layer that develops at the electrode–electrolyte interface. Another significant pathway involves redox (faradaic) reactions occurring on the electrode surfaces. Furthermore, supplementary mechanisms—including ion

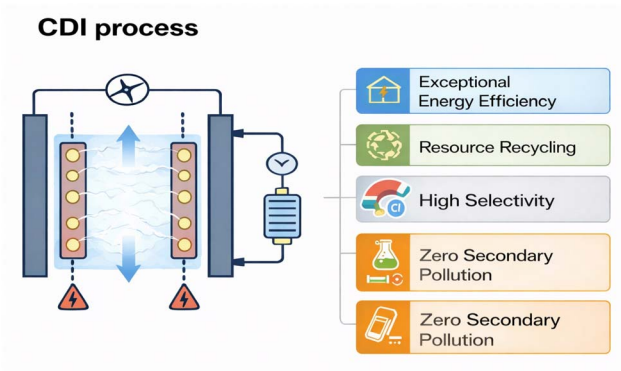

Fig. 2 Schematic of the CDI process and key performance metrics.

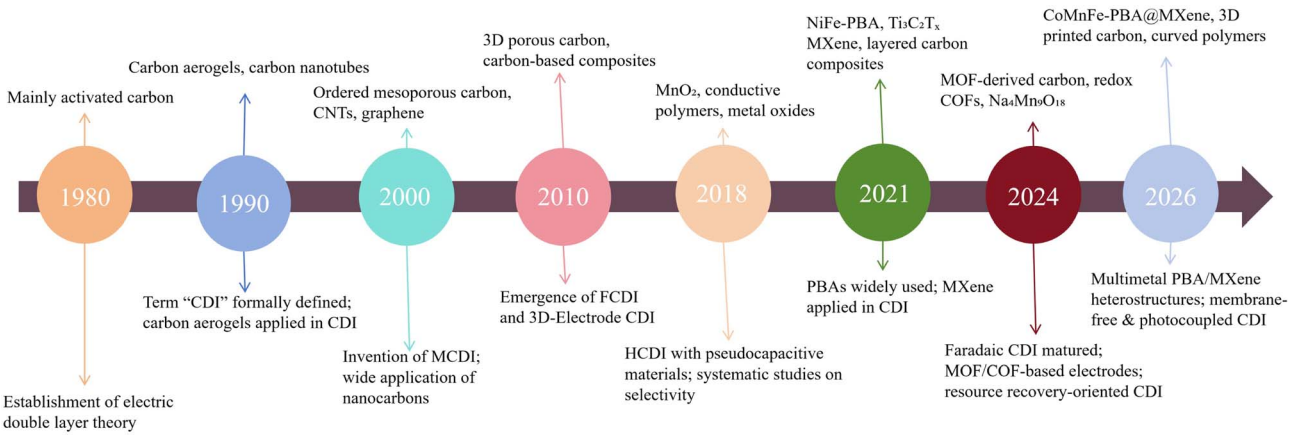

Fig. 1 Historical timeline for the development of CDI technology.

exchange, where target anions bind to specific functional groups on the electrodes, and complexation reactions—can also contribute to the overall ion removal efficiency.

2.1.1. EDL adsorption mechanism. EDL mechanism represents the classic and core operating principle of CDI technology. It functions by establishing a stable EDL at the electrode–electrolyte interface, enabling the physical adsorption of ions.[31] Porous carbon electrodes such as those derived from activated carbon, carbon nanotubes and graphene-based materials possess high specific surface areas and well-developed pore networks,[32,33] which are crucial for facilitating substantial EDL formation. When a low voltage is applied, anions (*e.g.*, fluoride (F^-), chloride (Cl^-), phosphate (PO_4^{3-})) are electrostatically attracted to the positively charged anode, while cations migrate to the negatively charged cathode,[34,35] resulting in the reversible adsorption and temporary storage of ions.

This EDL-based process is highly reversible and generally non-destructive to the electrode architecture. For instance, conventional activated carbon electrodes in a basic CDI cell can typically undergo more than 50 adsorption–desorption cycles.[36,37] The adsorbed ions can be released by short-circuiting the electrodes or applying a reverse voltage, after which the electrode's porous structure and adsorption capacity remain largely intact. However, a significant limitation of the pure EDL mechanism is its inherent lack of ion selectivity. Its performance is predominantly governed by the physical properties of ions, such as their hydrated radius and charge.[24,38] For example, in water containing multiple anions, smaller Cl^- ions often outcompete F^- for adsorption sites.[39] Similarly, PO_4^{3-} typically exhibit lower adsorption affinity compared to Cl^- or F^- in PO_4^{3-}-rich water, owing to their higher charge density and larger hydrated radius.[40,41] This limited selectivity constrains the effectiveness of the EDL mechanism alone for treating complex water matrices that require the targeted removal of specific harmful anions. Consequently, it often needs to be integrated with functionalized electrodes to achieve enhanced ion-specific removal.

2.1.2. Faradaic redox mechanism. To address the limited selectivity of conventional EDL adsorption, the faradaic mechanism relying on reversible redox reactions is commonly employed in modified CDI electrodes.[42,43] Unlike EDL adsorption, which depends solely on electrostatic forces, this approach utilizes active components within the electrode to undergo specific and reversible chemical transformations under an applied electric field, enabling highly selective capture and release of target anions from mixed-ion solutions. For Cl^- removal, silver-based electrodes are effective for treating textile wastewater with high Cl^- concentrations (1000–3000 mg L^{-1}).[44,45] Cl^- is captured through the reversible oxidation of Ag to AgCl during the adsorption phase, forming a strong chemical bond. Subsequently, applying a reverse voltage reduces AgCl back to Ag, releasing the Cl^- into a concentrated stream.[46] For F^- removal from semiconductor wastewater, CeO_2-based electrodes are utilized, leveraging the redox cycling between Ce^{3+} and Ce^{4+} states.[47,48] The higher-valence Ce^{4+} species can exchange oxygen with F^-, forming stable Ce–F bonds, and the process is reversed during regeneration, maintaining high F^- selectivity even in the presence of Cl^- at 50-fold higher concentrations. Similarly, ZrO_2-based electrodes target PO_4^{3-} in fertilizer wastewater, where Zr^{4+} ions undergo reversible interactions to form stable complexes with PO_4^{3-}, preferentially adsorbing it over competing ions.[49,50]

Compared to EDL adsorption, the faradaic mechanism can significantly enhance both selectivity and adsorption capacity. For instance, silver-based electrodes have demonstrated Cl^- adsorption capacities as high as 156.4 mg g^{-1} with 90.8% capacity retention after 120 cycles.[51,52] However, key challenges remain, including the need to suppress side reactions. The applied voltage must be maintained below the thermodynamic threshold for water electrolysis (~1.23 V) to avoid energy-wasting water splitting. Additionally, electrode surfaces are often coated with conductive layers to mitigate structural degradation of the porous substrate during long-term operation, ensuring performance stability in practical water treatment applications.[53,54]

2.1.3. Synergistic mechanisms. Two synergistic mechanisms play vital roles alongside the classic EDL adsorption and faradaic redox reactions, collectively enhancing anion removal efficiency.[55,56] Reversible ion exchange, commonly exploited in functionalized electrodes, involves the reversible exchange of target anions with functional groups or exchangeable ions on the electrode surface, thereby improving selectivity. For instance, graphene/hydroxyapatite (HAP) composite electrodes remove F^- from groundwater by exchanging surface hydroxyl groups (–OH) of HAP with F, achieving over 90% F^- removal.[27,57] Similarly, La-based composite electrodes treat F^--contaminated industrial wastewater, where positively charged amino groups attract F^-, and hydroxyl groups further strengthen adsorption *via* ion exchange mechanism, maintaining >85% removal efficiency even with a ten-fold excess of Cl^-.[27] This mechanism also applies to other anions. For Cl^- removal from textile wastewater, Fe_3O_4/AC composite electrodes utilize hydroxyl groups on Fe_3O_4 to exchange with Cl^-, mitigating sulfate interference.[58,59] Likewise, ZrO_2/PPy composite electrodes target PO_4^{3-} in agricultural runoff; the surface ion exchange between hydroxyl groups on ZrO_2 and PO_4^{3-}, coupled with the attraction by positively charged amino groups in PPy, delivers an adsorption capacity of 28.5 mg g^{-1} PO_4^{3-} and stable performance over 50 cycles.[60–62] Complexation, another synergistic mechanism, relies on specific coordination between metal active sites on the electrode and target anions, enhancing separation in complex matrices.[63] La-based hydroxyapatite/3D graphene (LaHAP/3D-rGO) electrodes preferentially remove F^- from semiconductor wastewater *via* stable bonding at La^{3+} sites, even in the presence of competing nitrate.[27,58] Zirconium-based MOF-derived electrodes exhibit a strong affinity for F^-, where Zr^{4+} ions tightly bind F^-, reducing its concentration from 50 mg L^{-1} to below the 1.5 mg L^{-1} WHO limit.[64,65] Silver-doped nitrogen-rich carbon electrodes capture Cl^- through the formation of stable Ag–Cl bonds at Ag active sites, achieving a capacity of 142 mg g^{-1} and a 3.8-fold selectivity for Cl^- over other ions.[44,66,67] Iron-nitrogen coordinated porous carbon electrodes target PO_4^{3-} in fertilizer wastewater, where Fe-N_x sites form stable complexes with PO_4^{3-}, ensuring its preferential capture over NO_3^-.

Overall, the ion removal mechanism in CDI is recognized to have evolved from a reliance on single EDL adsorption to a multi-mechanism system encompassing EDL, redox, ion exchange, and complexation.[20,68] The effectiveness of each pathway depends on electrode design, target ion properties, and operating conditions. To balance synergistic effects and energy efficiency, operating parameters are typically optimized within ranges of 0.8–1.2 V and 10–20 mL min^{-1}.[65] The central optimization objective is to enhance the specificity of each mechanism, reduce competitive adsorption, and minimize side reactions.[69] This integrated mechanistic framework provides crucial theoretical support for the efficient and selective removal of anions like F^-, Cl^-, and PO_4^{3-} in real-world applications.

2.2. Advantages of CDI technology

CDI technology presents a key solution for addressing various anionic pollutants, stemming from three key advantages:[70] low energy consumption, high selectivity for specific anions, and environmental friendliness.[71] Firstly, CDI operates with significantly lower energy consumption compared to conventional processes like RO, substantially reducing long-term operational costs. Secondly, it can achieve high selectivity for target anions even in complex water matrices.[70,72] For instance, silver-modified electrodes exhibit a 3.8-fold higher selectivity for Cl^- over sulfate,[44,73] and Zirconium oxide-based tailored materials prioritize PO_4^{3-} capture with capacities up to 32.7 mg g^{-1} PO_4^{3-}, while lanthanum-based composites maintain F^- removal efficiency above 90% even with a 50-fold excess of Cl^-.[27,58] Thirdly, CDI is environmentally benign; its operation requires no chemical additives, avoiding secondary pollution, and the electrodes show excellent reusability, retaining over 85% of their initial adsorption capacity after 50 cycles.[74] These advantages are underpinned by two fundamental innovations. The first is the integration of multiple electrochemical mechanisms: physical ion capture *via* EDL adsorption, selective binding through faradaic redox reactions, and enhanced stability/selectivity afforded by ion exchange or complexation.[75,76] The second is optimized material adaptability: porous carbon materials are well-suited for EDL adsorption, metal- or metal oxide-doped composites facilitate selective redox processes, and specialized materials such as MOF-derived structures significantly enhance the targeting capability for specific anions like F^- and PO_4^{3-}.[77,78]

2.2.1. High energy efficiency. CDI technology offers a distinct advantage in energy efficiency for removing anions such as F^-, Cl^-, and PO_4^{3-} from various wastewater streams.[79] Its energy consumption is significantly lower than that of conventional separation technologies. Under practical operating conditions, energy use can be as low as 0.037 kW h per cubic meter of treated water.[80,81] Even when processing high-concentration anion-containing wastewater (*e.g.*, Cl^--rich textile dyeing effluent or PO_4^{3-}-contaminated agricultural runoff), CDI typically maintains energy consumption below 0.08 kW h m^3, which is substantially lower than the demands of processes like ED, nanofiltration, electrocoagulation, and RO.[80,82,83] This low energy footprint can be attributed to two key factors. First, the applied electric field is used primarily to drive ion electrosorption and desorption, without inducing significant phase changes or sustaining energy-intensive side reactions.[84] Second, electrode regeneration is straightforward, requiring only system short-circuiting or the application of a low reverse voltage, which enables over 80% energy recovery during the regeneration step.[85] For example, silver-based electrodes for Cl^- removal recover energy when AgCl is reduced to Ag, and zirconium oxide-based electrodes for PO_4^{3-} capture maintain energy recovery efficiencies above 85% during regeneration.[44,45,86] Importantly, this regeneration does not require additional chemical reagents, further reducing operational costs and energy input. Furthermore, CDI systems typically achieve high water recovery rates exceeding 85%, markedly higher than those of RO (<70%) and nanofiltration (70–75%).[87,88] This characteristic makes CDI especially valuable in water-scarce contexts, such as treating F^--contaminated groundwater in arid regions, recycling chloride-laden cooling water in industrial parks, or processing PO_4^{3-}-rich agricultural runoff. By minimizing wastewater discharge and maximizing the yield of usable water, high-water-recovery CDI aligns well with the goals of sustainable water management for anion pollution control.

2.2.2. Selective ion removal capacity. The targeted removal of specific anions such as F^-, Cl^-, and PO_4^{3-} from complex water matrices *via* CDI is achieved through the rational functionalization of electrode materials.[89] F^-, prevalent in semiconductor wastewater and groundwater,[26,90] can be selectively captured by CDI electrodes with tailored affinity. LaHAP/3D-rGO composites maintain an 87% F^- removal rate even with a 50-fold excess of Cl^-. AC-based composites containing Al, Fe, and Ti oxides (AC-$Al_4Fe_{2.5}Ti_4$) reduce F^- concentration in natural water from 5.15 mg L^{-1} to 1.18 mg L^{-1}.[90] Fe–N–C single-atom catalysts (FeN_x/C) leverage the synergy of FeN_3 and FeN_4 sites to achieve a high F^- adsorption capacity of 158.33 mg g^{-1},[26,91] demonstrating good tolerance towards coexisting CO_3^{2-} and NO_3^{2-}. For Cl^-, a common pollutant in textile and food processing effluents, Ag/AgCl nanoparticles anchored on $Ti_3C_2T_x$MXene (Ag/AgCl/$Ti_3C_2T_x$) utilize Ag^+ active sites. This design delivers a Cl^- adsorption capacity of 156.4 mg g^{-1}, retains 90.8% capacity after 120 cycles, and exhibits a Cl^-/SO_4^{2-} selectivity factor of 3.8 in mixed-anion water.[92,93] PO_4^{3-}, originating from agricultural runoff and fertilizer wastewater, is effectively targeted by zirconium oxide-embedded nitrogen-doped porous carbon electrodes (ZrO_2@NC), where Zr^{4+} sites play a key role.[79] These electrodes achieve a PO_4^{3-} adsorption capacity of 32.7 mg(as P) g^{-1} and maintain over 80% removal efficiency even in the presence of a 20-fold excess of NO_3^-.[60] The high selectivity stems from the synergistic interplay of multiple mechanisms, which include electrostatic adsorption within the EDL, specific complexation, and ion exchange mechanisms.[94] F^- removal primarily involves the formation of stable inner-sphere complexes with Lewis acid metal centers like La^{3+} or Zr^{4+}, Cl^- capture is achieved through reversible redox complexation with Ag^+/Ag^0 couples. PO_4^{3-} uptake engages in ligand exchange with Zr^{4+} to form strong Zr–O–P bonds,[95,96] complemented by electrostatic attraction. This multi-mechanism approach effectively overcomes the inherent poor

selectivity of conventional pure carbon electrodes, which rely solely on physical adsorption,[97,98] thereby enabling the targeted removal of harmful anions in practical water treatment.

2.2.3. Operational stability and regenerability. CDI electrodes typically exhibit excellent cycling stability and regenerability, maintaining high adsorption capacities for F^-, Cl^-, and PO_4^{3-} over repeated adsorption–desorption cycles.[99] This exceptional durability is consistently evidenced across a range of functionalized materials tailored for different anions. Reduced graphene oxide/hydroxyapatite (rGO/HA) composite electrodes show no significant capacity loss after 50 cycles. AC-$Al_4Fe_{2.5}Ti_4$ electrodes maintain a desorption efficiency above 93.8% over 10 cycles, and FeN_x/C electrodes demonstrate stable performance over 100 cycles without apparent structural degradation.[27,57] In chloride capture, Ag/AgCl/$Ti_3C_2T_x$ electrodes preserve 90.8% of their initial Cl^- adsorption capacity after 120 cycles. Similarly, for PO_4^{3-} removal, ZrO_2-embedded nitrogen-doped carbon (ZrO_2@N–C) electrodes retain over 80% of their adsorption capacity after 50 cycles when treating agricultural runoff.[45,100] The regeneration of CDI electrodes is accomplished solely *via* electrochemical methods, such as short-circuiting the system or applying a mild reverse voltage, without the need for chemical reagents.[101] This reagent-free approach not only prolongs electrode service life but also eliminates the secondary pollution associated with chemical regeneration byproducts. Consequently, it contributes to lower long-term operational costs for water treatment systems designed to remove diverse anionic contaminants.[102,103]

2.2.4. Mild and flexible operation. CDI technology operates under mild conditions, requiring neither high temperature/pressure nor strongly acidic/alkaline environments.[104] The CDI electrode reactions function within a near-neutral pH range, thereby avoiding significant pH fluctuations in the treated water, which is beneficial for various anion-polluted sources like F^--contaminated groundwater, Cl^--rich textile effluents, and PO_4^{3-}-laden agricultural runoff.[105,106] The operational flexibility of CDI systems is reflected in three key aspects. First, the system architecture is relatively simple, enabling modular assembly and facile scaling, which allows adaptation to both small-scale drinking water purification and large-scale industrial wastewater treatment.[107] Second, critical operational parameters including applied voltage, flow rate, and pH can be dynamically adjusted in response to influent water quality.[108] For instance, a lower voltage may be applied for treating low-concentration F^- in groundwater, a higher voltage for high-concentration Cl^- in textile wastewater, and an optimized pH for PO_4^{3-} removal from agricultural runoff.[109,110] This adjustability makes CDI suitable for a variety of water sources, including simulated water, groundwater, and industrial wastewater. Third, CDI exhibits compatibility with a wide array of electrode materials. Porous carbons, metal oxides (*e.g.*, Fe_3O_4, ZrO_2), metal–organic frameworks (MOFs; *e.g.*, UiO-66, MIL-101), and MXenes (*e.g.*, $Ti_3C_2T_x$) all serve as viable material platforms. These can be further functionalized to meet specific removal requirements.[20,21,23] For example, carbon-based materials are often used for electric double layer adsorption, metal oxides and MOFs are tailored for selective F^-/PO_4^{3-} capture *via* complexation, and MXene-based composites can be designed for high-efficiency Cl^- removal.

2.2.5. Environmental friendliness. CDI technology demonstrates environmental benignity across key stages of its lifecycle, aligning with sustainable water treatment principles for removing anions like F^-, Cl^-, and PO_4^{3-} from various sources.[111] This friendliness is manifested in several aspects. Firstly, many electrode materials are synthesized *via* environmentally benign routes, such as using biomass-derived carbon or fabricating composite oxides through coprecipitation, minimizing the environmental footprint from production.[112] Secondly, during operation, CDI systems generate no secondary pollutants such as chemical sludge or concentrated brine residues that are typical of processes like chemical precipitation or RO.[113,114] The small volume of concentrated solution produced during electrode regeneration, for instance from treating F^--rich industrial wastewater or Cl^--laden textile effluent, is highly concentrated, facilitating its subsequent treatment or potential resource recovery.[115,116] Besides, the intrinsic safety of CDI electrodes contributes to long-term environmental compatibility. Electrode materials like Al/Fe/Ti composite oxides and La-based composites exhibit low toxicity, with metal leaching levels well below established safety limits. For example, reported chromium leaching is as low as 0.01 mg L^{-1}, iron leaching from FeN_x/C electrodes is below 0.6 μg L^{-1}, and zirconium leaching from ZrO_2-based materials is negligible.[117,118] This minimal leaching effectively mitigates the risk of secondary water pollution during prolonged system operation, underscoring the environmental sustainability of CDI technology.

The unique advantages of CDI become most evident in comparison to conventional water treatment methods. Fig. 3 illustrates a comparative overview of CDI, RO, IX, and ED across key performance and sustainability metrics. Compared to RO, which achieves high removal rates but with substantial energy input, significant brine discharge, and inherent non-selectivity, CDI offers a pathway for energy-efficient and selective ion capture with minimal waste streams.[80] In contrast to IX, which provides high selectivity but relies on chemical regeneration that generates secondary waste and continuous operational costs, CDI achieves comparable selectivity through electrochemically reversible processes that require no added chemicals. While ED shares the electrochemical nature of CDI and enables continuous operation, it typically operates at higher voltages and is more susceptible to membrane-related challenges like fouling and scaling.[119] As elaborated above, CDI technology is distinct in combining low operational energy, tunable high selectivity through rational electrode design, and environmental friendliness from chemical-free operation.[120] This makes CDI not a universal substitute for mature technologies, but a highly competitive and complementary solution for targeted applications, especially selective removal of specific anions from moderate-salinity water where energy efficiency, minimal chemical use, and precise ion control are critical.

2.3. CDI configurations

To address the purification demands of complex water matrices, CDI technology has evolved from traditional symmetric electrode configurations to multifunctional designs,

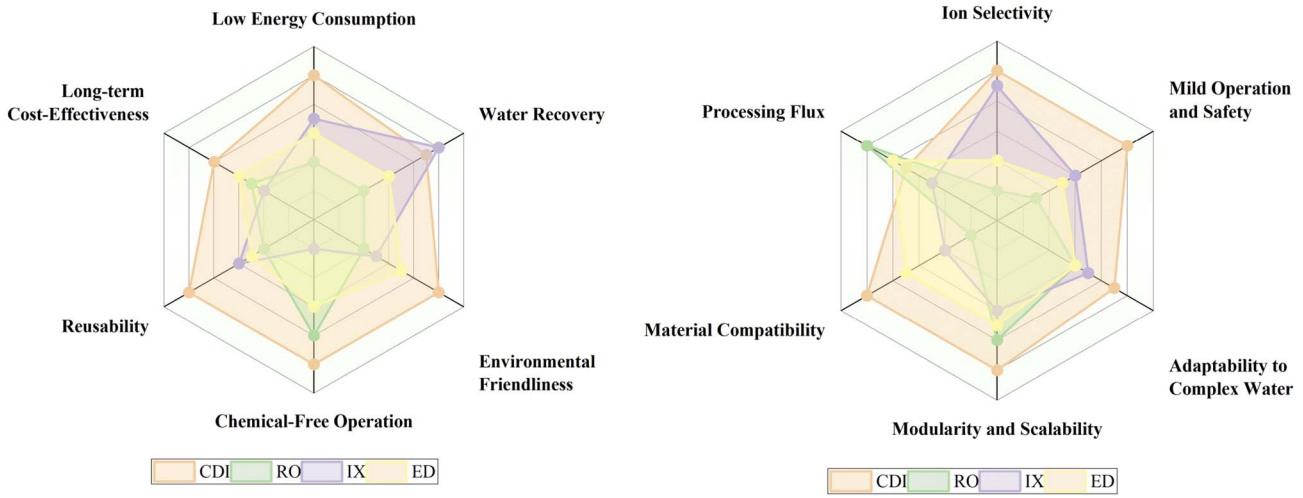

Fig. 3 Performance comparison of CDI technology against RO, IX, and ED approaches across technological and sustainability dimensions.

including membrane-coupled, hybrid electrode, and flow-electrode architectures. CDI configurations can be broadly categorized into the following five main types based on their architectural and operational principles (Fig. 4).[121]

2.3.1. Symmetric capacitive deionization (S-CDI). The S-CDI configuration represents the most basic CDI configuration. It relies solely on EDL adsorption without ion-exchange membranes (IEMs), which results in low cost and operational simplicity but offers limited ion selectivity. Consequently, it is primarily suitable for the preliminary desalination of low-salinity water, such as brackish water. The S-CDI system comprises a pair of parallel symmetric electrodes, current collectors, and an intermediate flow channel.[122] Under a low applied voltage (0.4–1.2 V), the electric field drives the feed water through the inter-electrode channel, where ion adsorption occurs *via* the formation of an EDL.[123,124] Specifically, the electric field directs anions in the water toward the anode, while cations migrate to the cathode. Relevant anions include F^- originating from groundwater, Cl^- from low-salinity textile wastewater, and PO_4^{3-} from dilute agricultural runoff. Concurrently, the CDI electrodes facilitate EDL formation, thereby enabling physical adsorption.[19] Owing to its structural simplicity, low manufacturing cost, and ease of operation, the S-CDI configuration is widely used.[125] Its efficacy under tested conditions is evidenced by the following: using activated carbon electrodes at 1.2 V with an initial F^- concentration of 10 mg L^{-1}, a 94.2% F^- removal rate was achieved from simulated water; at 1.0 V with an initial Cl^- concentration of 500 mg L^{-1}, an 89.5% Cl^- removal rate was obtained from low-salinity textile wastewater; and at 0.8 V with an initial PO_4^{3-} concentration of 5 mg L^{-1} (as P), an 85.3% PO_4^{3-} removal rate was attained from dilute agricultural runoff.[57,79]

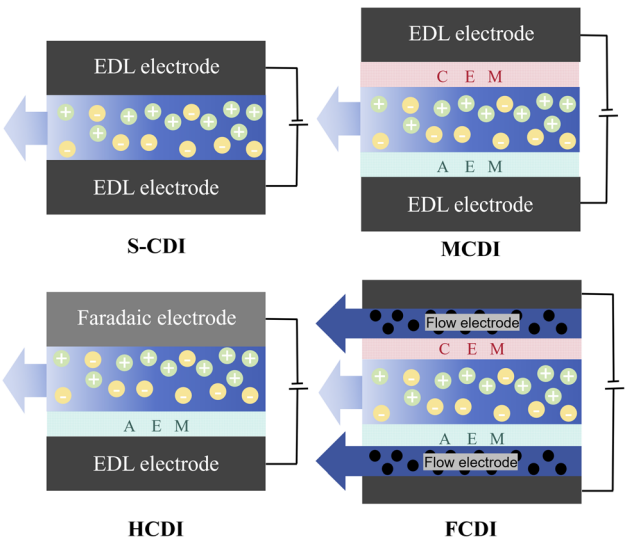

Fig. 4 Schematic illustrations of fundamental CDI configurations.

2.3.2. Membrane capacitive deionization (MCDI). The MCDI configuration enhances S-CDI by incorporating IEMs, introducing a membrane-based sieving mechanism that effectively suppresses co-ion expulsion. The synergy between EDL adsorption and membrane selectivity leads to a significant boost in adsorption capacity (40–60%) and much-improved ion selectivity, albeit at a higher cost and complexity compared to S-CDI. Specifically, MCDI optimizes the conventional S-CDI by incorporating IEMs between the electrodes and the flow channel, forming a layered structure of anode → anion exchange membrane (AEM) → flow channel → cation exchange membrane (CEM) → cathode,[126] in which AEMs permit exclusive anion transport and CEMs enable selective cation migration. This membrane-integrated architecture combines EDL adsorption with membrane-based sieving, effectively suppressing co-ion back-migration.[127] For instance, AEMs positioned at the anode side block the reverse diffusion of anions such as F^-, Cl^-, and PO_4^{3-} while directing target ions toward the respective electrodes. In MCDI configuration, F^- from groundwater traverses the AEM for anodic capture.[110,128] Cl^- from textile dyeing wastewater migrates across the AEM for selective

adsorption, and PO_4^{3-} from agricultural runoff, after passing through the AEM, is retained at the anode. Concurrently, cations including Na^+ and Ca^{2+} migrate through the CEM to the cathode, substantially reducing ion rediffusion losses.[129,130] This membrane integration directly translates into enhanced performance. Higher adsorption capacity arises from the synergistic effect of EDL adsorption and membrane selective sieving, with reported increases of 40–60% compared to conventional S-CDI.[131] An activated carbon electrode-based MCDI configuration can achieve 92.3% Cl^- removal from textile wastewater with 81.5% water recovery,[132] and a ZrO_2-modified MCDI configuration can reach 90.1% PO_4^{3-} removal from agricultural runoff (initial concentration 8 mg L^{-1} as P) with water recovery exceeding 80%.[133] Beyond capacity, the MCDI configuration also enhances ion selectivity, where the incorporation of monovalent anion-selective membranes effectively reduces competitive adsorption between multivalent and target anions.[134,135]

2.3.3. Hybrid capacitive deionization (HCDI). The HCDI configuration holds a distinct position due to its combination of mechanistic complexity and selective performance. The asymmetric pairing of an EDL electrode with a faradaic electrode creates a synergistic dual-mode capture system: the EDL component enables bulk ion capture, while the faradaic electrode provides chemical binding for target-specific retention. The integration of faradaic reactions improves charge efficiency, reflected in the configuration's excellent long-term cycling stability. Certain variants integrate IEMs to enhance performance[136] especially when treating water contaminated with F^-, Cl^- or PO_4^{3-}. In terms of its operating principle, the HCDI configuration operates *via* the coupled mechanisms of EDL adsorption and faradaic reactions. The faradaic electrode can bind target anions, for instance *via* La^{3+} sites for F^-, Ag^+ sites for Cl^- and Zr^{4+} sites for PO_4^{3-},[137] while the EDL electrode facilitates ion migration and maintains charge neutrality.[138] Furthermore, the HCDI configuration consistently delivers robust cyclic stability. For example, the Bi/rGO//AC HCDI cell retains over 90% F^- desorption after 10 cycles,[61,139] the Ag/AgCl//AC HCDI cell maintains 88% of its Cl^- capacity after 20 cycles, and the ZrO_2@N–C//AC HCDI cell sustains its PO_4^{3-} removal efficiency after 30 cycles.[140]

2.3.4. Flow capacitive deionization (FCDI). The FCDI configuration distinguishes itself from conventional CDI configurations through the use of suspended flow electrodes instead of fixed ones. These flow electrodes are composed of conductive particles dispersed in an electrolyte,[141] circulating between the electrode chamber and a storage tank *via* a pump. Ion-exchange membranes installed in the flow channel prevent electrode particle leakage and enable effective ion screening.[142] FCDI configuration operates on the principle of dynamic adsorption coupled with continuous ion removal. As the flow electrodes circulate through the system, they actively capture target anions from the influent.[97] Upon saturation, they are directed to the storage tank, where a mild applied voltage triggers electrochemical regeneration desorbing the adsorbed ions and restoring the electrodes' adsorption capacity.[143] This continuous operational mode confers several inherent advantages, it circumvents the saturation constraints of fixed-electrode systems, rendering FCDI particularly suitable for high-concentration anion wastewater (*e.g.*, with F^- levels exceeding 100 mg L^{-1}), it underpins a treatment capacity 3–5 times higher than that of MCDI configuration, positioning it as efficient for large-volume and high-pollution sources,[144,145] and its modular architecture enables flexible scale-up to accommodate diverse treatment requirements, from small-scale industrial wastewater to large-scale water treatment. Studies have demonstrated that FCDI maintains stable F^- removal efficiency above 85% during continuous treatment of fluorine-containing brackish water.[146,147] The ability to regenerate flow electrodes in batches within the storage tank without system shutdown simplifies operational procedures, reduces downtime, and enhances the overall continuity and reliability of the water treatment system.[148,149]

2.4. Key performance metrics

A critical assessment of CDI performance is essential for comparing different material designs, configuration architectures, and operational strategies. This section defines the key performance metrics universally employed to benchmark the efficacy of CDI for targeted ion removal.[150]

2.4.1. Ion electrosorption capacity (IEC). The IEC is a fundamental parameter for evaluating the ion removal.[151] This parameter represents the mass of ion removed relative to the mass of the active electrode material. It is quantified as the amount of ions adsorbed per gram of electrode material (in milligrams) and is determined using formula (1):

$$\mathrm{IEC} = \frac{(C_0 - C_e) \times V}{m} \quad (1)$$

where C_0 refers to the initial concentration of the feed solution, while C_e indicates the effluent concentration at the end of the adsorption phase. V denotes the volume of the treated solution, and m represents the mass of the active material in the working electrode (s). The IEC is directly governed by the intrinsic properties of the CDI electrode, which include critical factors such as specific surface area, redox activity, surface chemistry, and electrical conductivity. Moreover, operational conditions like the applied voltage, hydraulic residence time, initial ion concentration, and co-existing ions also have a significant impact on the IEC value.

2.4.2. Average ion electrosorption rate (AIER). The AIER quantifies the speed of ion removal relative to the mass of the electrode material. It is defined as the achieved IEC divided by the duration of the adsorption phase, with units of milligrams per gram per minute (mg g^{-1} min^{-1}),[150] and is determined using formula (2):

$$\mathrm{AIER} = \frac{\mathrm{IEC}}{t} \quad (2)$$

where IEC refers to the ion adsorption capacity obtained at the end of the adsorption phase, as calculated by formula (1), and t denotes the duration of the adsorption phase. AIER is linked to the processing throughput of the CDI system and is regarded as

a critical metric for assessing the feasibility for rapid water treatment applications.

2.4.3. Charge efficiency (CE). The CE is a key electrochemical parameter for evaluating the electrical efficiency of the ion removal process in CDI. This parameter represents the ratio of the electrical charge effectively utilized for ion adsorption to the total electrical charge passed through the CDI system.[131] It is defined as the ratio of the charge corresponding to the adsorbed ions to the total charge passed during the adsorption phase, typically expressed as a percentage, and is determined using formula (3):

$$\mathrm{CE} = \frac{q_{\mathrm{ads}}}{Q_{\mathrm{total}}} \times 100\% \quad (3)$$

In this equation, q_{ads} denotes the charge corresponding to the adsorbed ions, which can be calculated from the measured SAC *via* Faraday's law. Q_{total} represents the total charge passed during adsorption, obtained by integrating the current over time. The magnitude of CE is influenced by several factors, including the electrochemical properties of the electrode materials, the presence of ion-exchange membranes, and the occurrence of competing reactions such as water electrolysis. In CDI systems without ion-exchange membranes, the expulsion of co-ions can also lead to a reduction in CE. An ideal CE of 100% signifies that all charge passed is used for ion adsorption. In practical applications, a high CE is desirable as it correlates with lower energy consumption and is therefore an important indicator of the overall efficiency and economic viability of a CDI system.

2.4.4. Specific energy consumption (SEC). The SEC quantifies the electrical energy consumed to achieve a unit of ion removal performance. It is defined as the ratio of the total electrical energy input to either the volume of purified water produced or the mass of ion removal, with common units of kilowatt-hours per cubic meter (kW h m^{-3}) or per kilogram of ions removed (kW h kg^{-1}),[83] and is determined using formula (4):

$$\mathrm{SEC} = \frac{E_{\mathrm{total}}}{(V_{\mathrm{p}} \times \Delta C)} \quad (4)$$

where E_{total} denotes the total electrical energy consumed during a full adsorption–desorption cycle, typically obtained by integrating the power over time, V_{p} represents the volume of product water, ΔC is the average reduction in ion concentration. The SEC is primarily governed by the CDI system's electrochemical and operational efficiency, which includes factors such as the electrode's charge efficiency, internal resistance of the cell, and the energy recovery capability during regeneration.

2.4.5. Ion selectivity (separation factor, α). α is a paramount performance parameter for evaluating targeted remediation capability in CDI systems,[152] which is defined as the ratio of the distribution coefficients of the target ion to a competing ion between the electrode surface and the bulk solution, and is determined using formula (5):

$$\alpha_{(A/B)} = \frac{(q_A/C_{e,A})}{(q_B/C_{e,B})} = \frac{(q_A \times C_{e,B})}{(q_B \times C_{e,A})} \quad (5)$$

where $\alpha_{(A/B)}$ denotes the selectivity of target ion A over competing ion B, q_A and q_B are the adsorption capacities (or surface concentrations) of ions A and B on the electrode at equilibrium, respectively, and $C_{e,A}$ and $C_{e,B}$ represent the equilibrium concentrations of ions A and B in the bulk solution. Alternatively, selectivity can be pragmatically reported as the simple ratio of the adsorption capacities (q_A/q_B) or the removal efficiencies of the two ions under mixed conditions.[153] A high selectivity factor is essential for the efficient CDI operation in complex and multi-component water matrices and is regarded as the decisive metric for assessing the technology's suitability for precision separation and targeted pollutant removal.

These key performance metrics are interdependent, and optimizing a CDI system often involves balancing trade-offs among them. For instance, a material may achieve a high IEC at the expense of charge efficiency, leading to a higher SEC. Similarly, exceptional selectivity for a target ion might correlate with a lower overall adsorption rate.[154] Therefore, the choice of CDI electrodes, configuration, and operating conditions must be strategically aligned to prioritize the metrics most critical for a given application, whether the goal is achieving ultra-low contaminant concentrations, minimizing energy and chemical usage, or maximizing water yield.

3. CDI electrode materials

The performance of CDI technology, which encompasses its ion adsorption capacity, ion selectivity, charge efficiency, and long-term stability, is fundamentally dictated by the architecture and chemistry of its electrode materials.[155] This chapter adopts a material-centric perspective to systematically examine the design principles, functional mechanisms, and evolutionary trajectory of electrode systems engineered for CDI, particularly in the context of targeted anion removal. The field has progressed from early reliance on porous carbons for non-selective electrosorption toward the rational design of functional materials that engage target ions through specific interactions. This evolution reflects a shift from viewing the electrode as a generic adsorbent to designing it as a precision tool, with material properties tailored to overcome the distinct challenges posed by different anionic pollutants.

3.1. Carbon electrode materials

Carbon materials constitute the foundational CDI electrode operating primarily through the formation of an EDL. Their performance is governed by key structural parameters: a high specific surface area (often exceeding 1000 $m^2\ g^{-1}$) to maximize ion-accessible sites, a hierarchical pore network, and high electrical conductivity to ensure efficient charge distribution.[156] Carbon electrodes offer compelling advantages, including low cost, mature manufacturing processes, and excellent electrochemical stability over thousands of cycles. Their principal limitation, however, is the inherent lack of ion specificity stemming from the non-faradaic and physical nature of EDL adsorption.[156] In complex ionic matrices, this results in competitive adsorption where capacity is consumed by non-

target ions, severely restricting selective ion removal efficiency. While indispensable as conductive scaffolds and baseline materials, pure carbons are often insufficient for applications demanding high selectivity. Their primary role has thus evolved to serve as robust and conductive matrices in composite materials where they support and synergize with more selective functional components.[20]

3.2. Faradaic electrode materials

To overcome the selectivity limitations inherent to carbon electrodes, faradaic electrode materials are widely employed. These are categorized by their dominant interaction modes, including inner-sphere complexation, which utilizes hard Lewis acid metal centers such as La^{3+} and Zr^{4+} to form stable complexes with anions like F^- and AsO_4^{3-}.[157] Reversible redox-based materials, exemplified by the Ag/AgCl couple for selective Cl^- capture, where capacity is directly tied to redox charge and nanostructural design is critical for stability.[158] Ligand-exchange-driven materials, which rely on geometric and electronic complementarity between high-valence metal cations Zr^{4+} and Fe^{3+} and polyvalent oxyanions like phosphate to address selectivity in competitive matrices.[159] Conducting polymers especially polyaniline (PANI), whose tunable doping/dedoping behavior allows affinity modulation *via* functional groups and oxidation states.[160] However, the practical deployment of these functional materials is counterbalanced by synthesis and stability challenges, including precursor cost, the need for scalable production methods, and the imperative to maintain structural and chemical integrity of active sites over extended cycling to prevent leaching or deactivation.[161]

3.3. Composite electrode architectures

The most significant advances in CDI electrodes have emerged from composite architectures that integrate multiple materials to achieve synergistic properties unattainable by any single constituent.[162] The dominant strategy involves fabricating carbon- or MXene-based functional composites, where a conductive backbone serves as an efficient electrical highway and robust mechanical framework, while dispersed nanoparticles or atomically dispersed sites provide selectivity. Examples like FeN_x/C for F^- removal or Ag/AgCl/MXene for Cl^- removal demonstrate the carbon or MXene component mitigates the poor intrinsic conductivity of the active phase, while FeN_x and Ag/AgCl provide excellent selective anion adsorption.[57] Similarly, composites incorporating layered double hydroxides (LDHs) with conductive carbon matrices, namely CoAl-LDH/C, successfully combine the high anion exchange capacity of LDHs with the necessary electrical pathways of the carbon matrix, enabling efficient electrosorptive removal of PO_4^{3-}.[163] Collectively, the composite approach yields electrodes with significantly enhanced conductivity, which ensures full utilization of active sites for ion capture. This synergistic design not only lowers the kinetic barrier for ion diffusion but also enables efficient charge transport throughout the composite electrode for ion capture.[164]

4. Targeted anion removal

4.1. F^-, Cl^-, and PO_4^{3-} removal

The development of CDI technologies for anion removal is driven by stringent requirements for water quality in both industrial and municipal sectors. Among various anionic pollutants, F^-, Cl^-, and PO_4^{3-}, are of particular concern due to their distinct environmental and health impacts. However, their concurrent or selective removal presents a significant challenge, as their differing ionic radii, charges, and hydration energies necessitate tailored electrode design.

4.1.1. CDI technology for F^- removal. F^- predominantly occurs in rocks and soils as insoluble minerals such as calcium fluoride and fluorspar, whereas in natural water bodies, it exists primarily as free F^-. Its migration and transformation are governed by three key factors, water pH, coexisting ions (*e.g.*, Ca^{2+}, Mg^{2+}) and adsorption media in the aquatic environment.[165] F^- exerts a dual effect on human health. At moderate concentrations (0.5–1.0 mg L^{-1}), it promotes tooth enamel mineralization, enhancing resistance to acid erosion, thereby preventing dental caries. However, excessive F^- intake exceeding the WHO drinking water guideline of 1.5 mg L^{-1} can lead to fluorosis.[166,167] Long-term accumulation results in dental fluorosis and skeletal fluorosis, which in severe cases can cause bone deformities and kidney damage.[168,169] These health risks are exacerbated by anthropogenic F^- inputs from industrial activities, which discharge F^- at concentrations far exceeding natural background levels. In semiconductor fabrication, hydrofluoric acid is widely used for etching and cleaning silicon wafers; The resulting wastewater typically contains 50–200 mg L^{-1} of F^-, far above common discharge limits (*e.g.*, 10 mg L^{-1} in China's GB 8978–1996).[170,171] The substantial disparity between elevated industrial F^- concentrations and stringent discharge standards underscores the pressing need for efficient and economical F^- removal technologies.[172] Crucially, the presence of high concentrations of competing ions like Cl^- in many of these wastewaters makes selective F^- removal a paramount engineering challenge.

Considerable research has been conducted on CDI technology for F^- removal. Electrode modification plays a central role in enhancing defluoridation performance, with the introduction of metal active sites and the construction of composite structures serving as two primary strategies.[173,174] LaHAP/3D-rGO composite CDI electrodes demonstrate high selectivity in complex matrices. They maintain 87% F^- removal efficiency even in the presence of chloride ions that are 50 times more concentrated, while achieving an adsorption capacity of 54.4 mg g^{-1}.[27,175] Besides, FeN_x/C electrodes in CDI device achieve an ultra-high F^- adsorption capacity of 158.33 mg g^{-1} and exhibit pronounced tolerance to interfering ions (Fig. 5).[27,57,174] The exceptional capacity stems from the atomically dispersed Fe-N_x sites, which form strong complexes with F^-. Importantly, these single-atom sites are stabilized within the carbon matrix, minimizing Fe leaching and maintaining structural integrity during the faradaic process.[176]

The removal mechanism of F^- in CDI technology has progressed from a simple EDL adsorption process to a synergistic

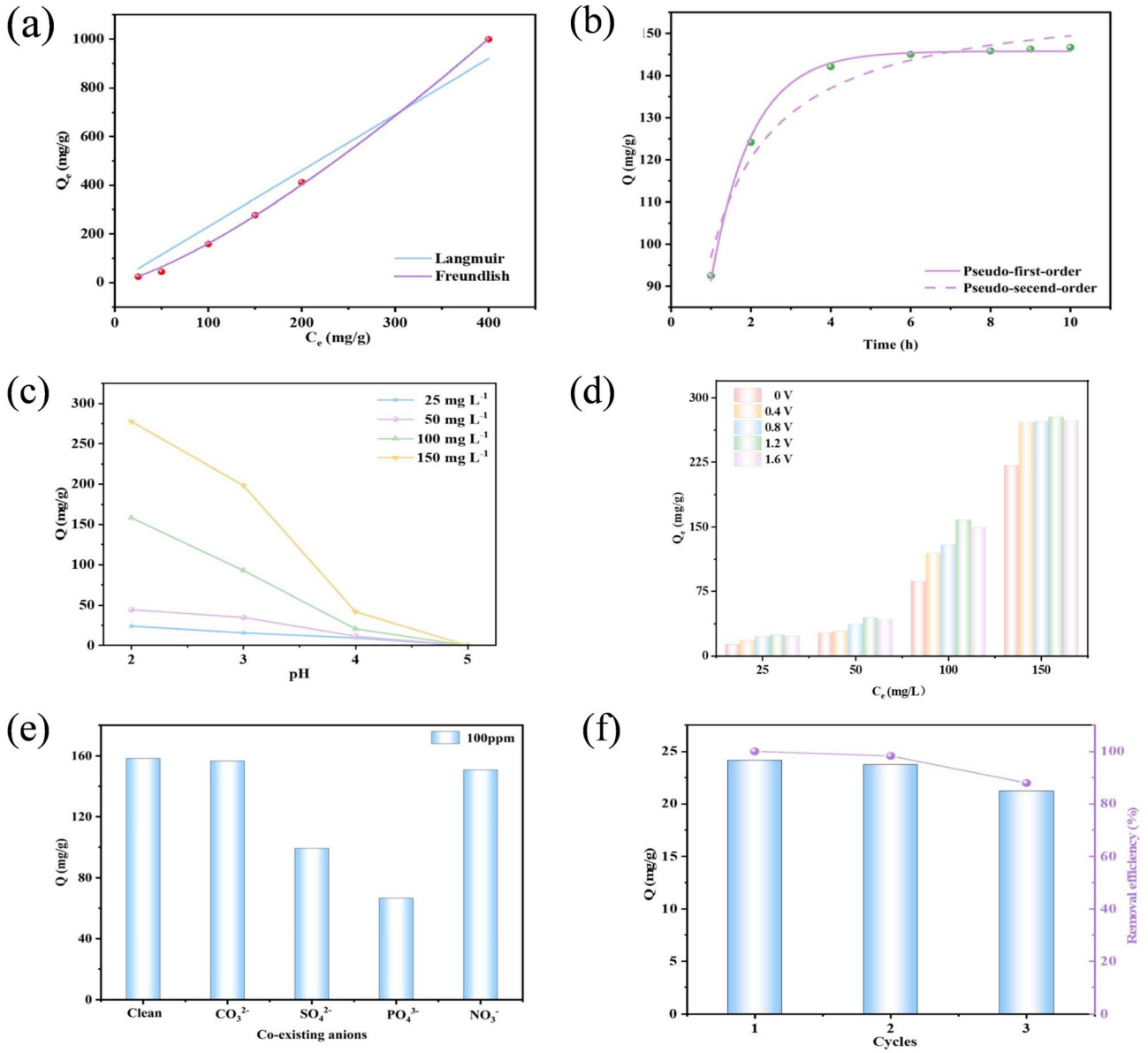

Fig. 5 Electrochemical adsorption performance of FeN_x/C electrodes for F^- removal. (a) Adsorption isotherms (Langmuir and Freundlich models) for F^- removal. (b) Adsorption kinetics of F^- onto the FeN_x/C electrode. (c) Effect of solution pH on F^- adsorption capacity. (d) Influence of applied voltage on F^- removal performance. (e) Selectivity of FeN_x/C for F^- in the presence of various competing anions. (f) Cycling stability of the FeN_x/C electrode over three consecutive adsorption–desorption cycles. (reprinted with permission from Separation and Purification Technology,[174] copyright 2024, Elsevier).

and multi-mechanism system that integrates EDL adsorption, faradaic redox reactions, and ion exchange/complexation (Fig. 6).[174] The left panel depicts the foundational EDL adsorption mechanism, where fluoride ions are non-selectively captured *via* electrostatic forces at the electrode interface. The right panel demonstrates the introduced faradaic pathway, where electrochemical reactions enable selective and high-capacity ion capture through chemical transformations. Metal-based active sites, such as La^{3+}, FeN_x, and Ce^{4+}, serve as the core drivers for selective F^- capture. These sites enable preferential adsorption either by forming stable inner-sphere complexes with F^- ions or through specific ion-exchange interactions.[177,178] This coordinated, multi-mechanism approach leverages the strengths of each pathway: EDL provides rapid ion enrichment, redox contributes to high-capacity capture, and ion exchange/complexation ensures specificity for F^- removal in complex waters.

4.1.2. CDI technology for Cl^- removal. Cl^- are among the most widely distributed anions in nature, occurring predominantly in dissolved form in seawater, brackish groundwater, and surface runoff.[179] Their prevalence is significantly amplified by anthropogenic activities, with key industries such as textile dyeing and food processing generating wastewater containing Cl^- concentrations typically ranging from 1000–

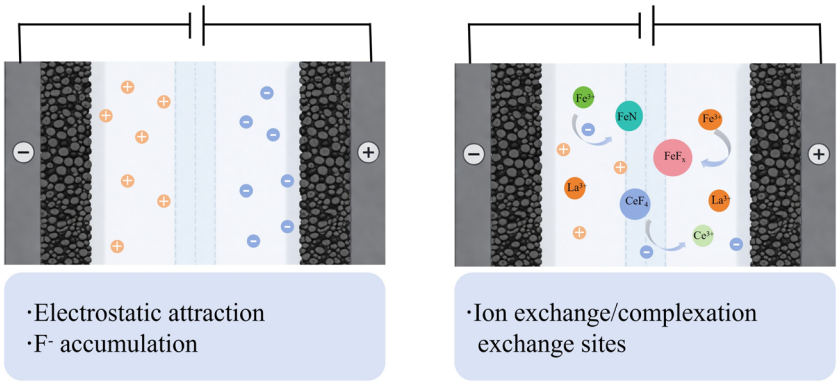

Fig. 6 F^- removal in CDI evolves from single EDL adsorption (left) to a synergistic multi-mechanism system (right) about ion exchange/complexation, such as metal-based sites (*e.g.*, La^{3+}, FeN_x, Ce^{4+}) enabling selective F^- capture.

5000 mg L^{-1}.[180,181] If discharged untreated, these effluents pose severe threats, they can induce soil salinization, reducing agricultural yields,[182,183] and act as vectors to enhance the mobility and toxicity of co-existing heavy metals.[184,185] For human health, long-term consumption of water with Cl^-exceeding the WHO guideline of 250 mg L^{-1} is associated with gastrointestinal issues and increased renal burden.[186–188]

The core strategy to overcome the limited capacity and selectivity of traditional carbon electrodes involves introducing functional components that engage Cl^- through specific interactions. The incorporation of reversible redox couples, such as the Ag/AgCl system, enables high-capacity ion capture through faradaic reactions, representing a strategy based on redox-active metal sites. For example, Ag/AgCl confined within MXene nanosheets achieves an exceptional Cl^- adsorption capacity of 156.4 mg g^{-1}.[189] The confinement structure is crucial for both performance and stability: it maximizes the utilization of redox-active Ag/AgCl sites and physically constrains them to prevent aggregation or detachment during continuous redox cycling.[190] Conductive polymer modification, exemplified by PANI coatings, introduces pseudocapacitance and ion-specific affinity to electrodes. For instance, a PANI-modified electrode operated at +0.35 V (*vs.* Ag/AgCl) achieves a high Cl^- adsorption capacity of ~65 mg g^{-1} with near-unity coulombic efficiency and pronounced selectivity for Cl^- over competing sulfate and PO_4^{3-} ions (Fig. 7).[23] In the context of composite materials, iron nanoparticle-embedded flexible carbon nanofibers achieve stable chloride removal (>88% efficiency) within FCDI systems, highlighting the adaptability of these engineered electrodes for continuous industrial-scale water treatment.[191,192] The high Cl^- adsorption performance observed in advanced CDI electrodes is founded on a synergistic mechanistic framework that integrates EDL adsorption for initial ion concentration, faradaic redox reactions for high-capacity, reversible capture, and specific complexation for enhanced selectivity in mixed-ion solutions.[193]

4.1.3. CDI technology for PO_4^{3-} removal. Excessive PO_4^{3-} input from anthropogenic activities, such as agricultural runoff (0.5–5 mg L^{-1} P^{-1}), industrial discharges (10–100 mg L^{-1} P^{-1}), and domestic sewage (5–20 mg L^{-1} P^{-1}), has become a primary driver of eutrophication.[194] This process, triggered when total phosphorus exceeds 0.02 mg L^{-1}, leads to harmful algal blooms, dissolved oxygen depletion, and severe ecological and economic damage, as evidenced in lakes like Taihu in China.[195,196] Beyond environmental harm, elevated PO_4^{3-} interferes with calcium absorption in humans and can corrode metal components in high-purity water systems for electronics manufacturing.[197]

Although conventional carbon-based CDI electrodes offer broad electrochemical compatibility, their intrinsic lack of specific affinity for PO_4^{3-} limits their practical utility in achieving low effluent concentrations required for regulatory compliance. To overcome this, recent strategies focus on incorporating metal centers that exhibit strong interactions with PO_4^{3-} ions, thereby enabling selective and efficient removal performance. The achieved cycling stability of CDI systems under realistic operating conditions, evidenced by less than 15% capacity decay after 20 cycles for ZrO_2-embedded nitrogen-doped porous carbon (ZNPC) electrodes (Fig. 8), indicates high adsorption capacities with structural integrity and minimal metal leaching even in complex matrices.[198,199] This robust cyclic performance is critical for scalable deployment, as it directly translates into reduced operational downtime, lower regeneration frequency, and extended electrode service life. Such benefits directly address the key economic and technical barriers that have historically hindered CDI adoption in large-scale wastewater treatment. As a result, this class of stable and selective CDI approach holds strong potential for application across diverse sectors: mitigating agricultural non-point source pollution by targeting residual phosphorus in surface runoff, treating high-concentration industrial effluents where PO_4^{3-} levels often exceed 10 mg L^{-1}, and enabling the production of high-purity process water for electronics and pharmaceutical industries.

Electrodes featuring Zr^{4+} sites, for instance, ZrO_2-embedded nitrogen-doped porous carbon derived from ZIF-8, achieve high PO_4^{3-} adsorption capacity, such as 32.7 mg P g^{-1}, by leveraging specific ligand exchange. This exemplifies the high-capacity performance of zirconium-based electrode materials.[190] The nitrogen-doped carbon matrix protects the ZrO_2 nanoparticles, while the strong Zr–O–P bonds formed during adsorption are reversible yet robust. Under near-neutral pH conditions, which

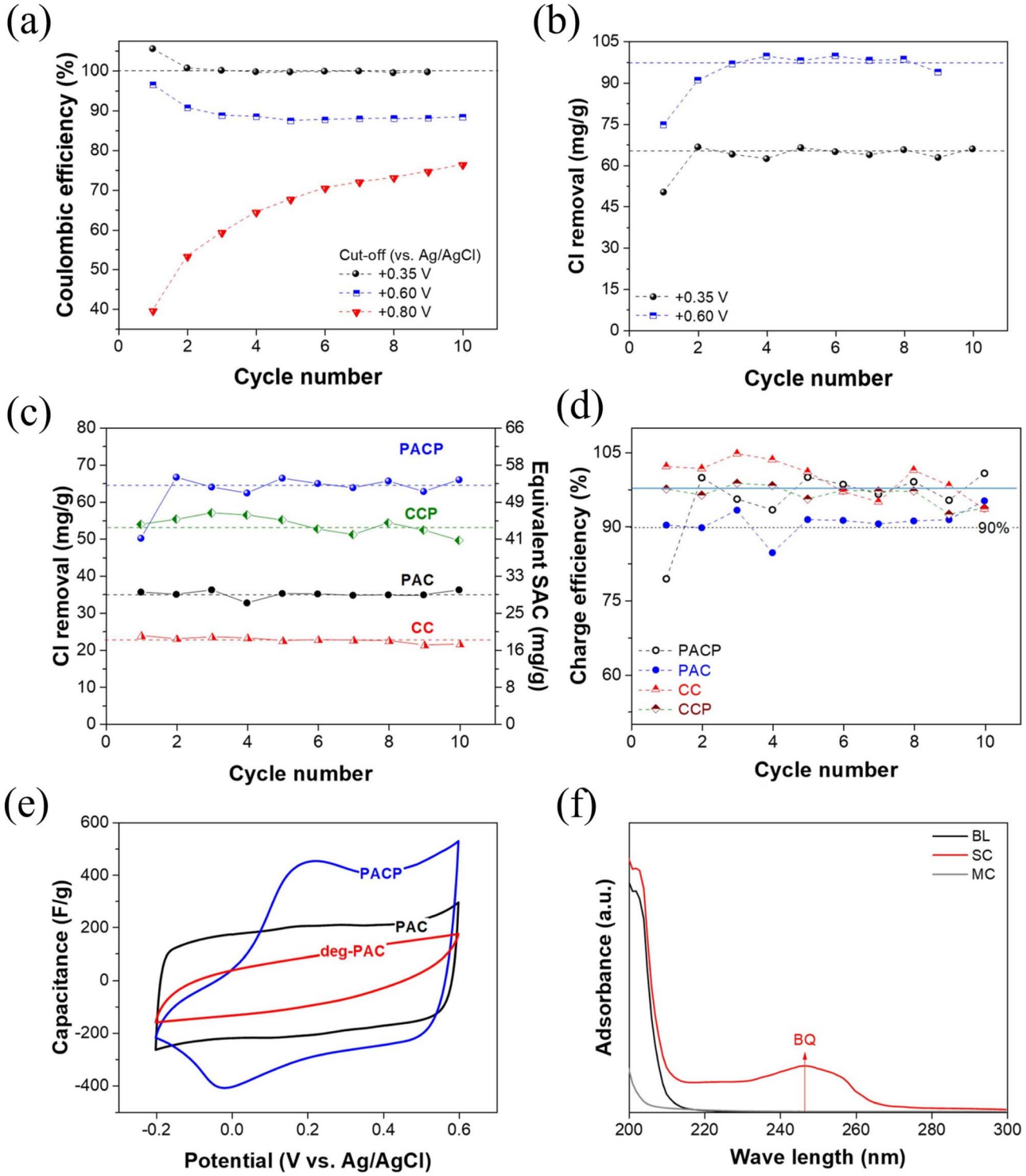

Fig. 7 Electrochemical stability and anion selectivity of PANI-modified CDI electrodes for targeted Cl^- removal. (a) coulombic efficiency over 10 cycles at different applied potentials. (b) Cl^- removal capacity during cycles. (c) Comparison of Cl^- removal capacity and charge efficiency for different electrodes (PACP, CCP, PAC, CC). (d) Long-term cycling stability over 10 cycles. (e) CV curves at 10 mV s^{-1} showing the capacitance behavior sof PACP, PAC, dig-PAC, and AC electrodes. (f) UV-Vis absorption spectra of BG (before graphitization) and IG (after graphitization) samples, indicating the structural transformation of the carbon material. (reprinted with permission from Separation and Purification Technology,[23] copyright 2022, Elsevier).

are optimal for both PO_4^{3-} adsorption and material stability, the electrode exhibits negligible Zr leaching and maintains over 80% of its adsorption capacity after 50 cycles in complex agricultural runoff. This underscores that the optimal adsorption condition is simultaneously a condition that favors material stability.[199,200] The CoAl-LDH/C composite as CDI electrode

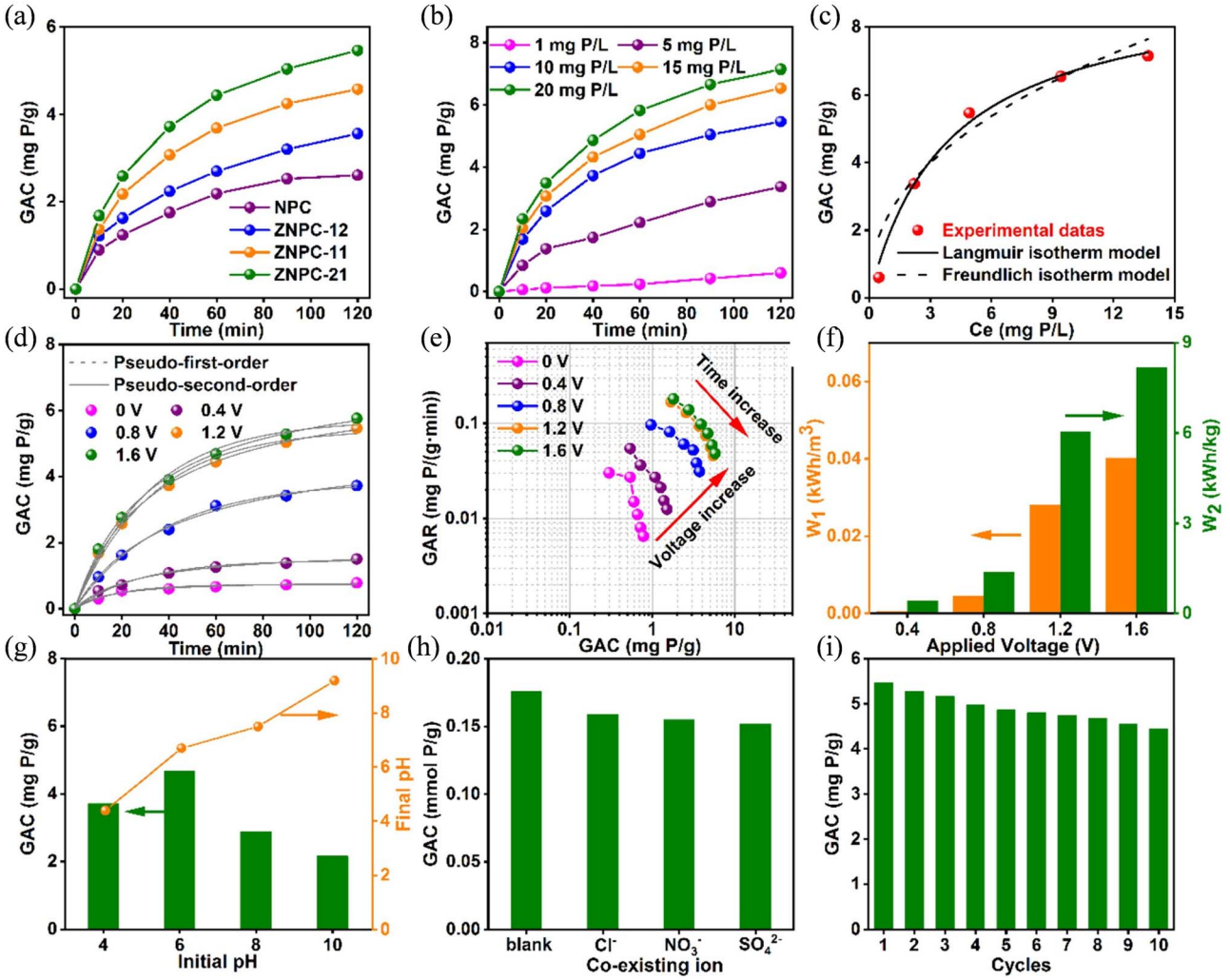

Fig. 8 Phosphorus removal performance and influencing factors of the NPC, ZNPC-12, ZNPC-11, ZNPC-21, electrodes. (a) Gravimetric adsorption capacity (GAC) of different electrodes over time. (b) Effect of initial phosphorus concentration on GAC. (c) Langmuir and Freundlich isotherm model fitting for phosphorus adsorption. (d) Effect of applied voltage on GAC. (e) Ragone plot (GAR *vs.* GAC) at different voltages. (f) Energy consumption per unit volume of treated water at different voltages. (g) Effect of solution pH on GAC and the corresponding final pH. (h) Effect of competing anions (Cl^-, NO_3^-, SO_4^{2-}) on phosphorus removal. (i) Cycling stability of the ZNPC-21 electrode over 10 adsorption–desorption cycles (reprinted with permission from Carbon,[199] copyright 2025, Elsevier).

combines the inherent anion exchange capacity of LDHs with the essential electrical conductivity provided by the carbon matrix. They demonstrate strong anti-interference ability, achieving a PO_4^{3-} selectivity factor of 2.6 in the presence of competing ions like sulfate and Cl^- (Fig. 9).[99] The layered structure of LDH provides structural stability and abundant sites. The conductive carbon backbone ensures electrical connectivity and mitigates the poor inherent conductivity of LDHs. This synergistic design enables the composite to maintain its structural integrity and ion-exchange capability over multiple cycles, which is essential for sustaining its selective PO_4^{3-} removal performance in long-term operation.[190]

Based on the above discussions, the advanced electrode materials discussed herein address key economic and technical barriers to real-world CDI implementation through three synergistic performance attributes. First, high anion adsorption capacity reduces the electrode volume needed to treat a given contaminant load, enabling compact and cost-effective modular systems for industrial use. Second, high anion selectivity ensures efficient operation in complex waters by preventing capacity waste on background ions, thereby extending operation cycles, reducing regeneration frequency, and improving overall efficiency. Third, robust adsorption stability encompasses both cycling performance and tolerance to interfering ions. Tolerance to common ions enhances operational robustness and reduces pretreatment needs, while exceptional regenerative stability prolongs electrode service life. This directly lowers electrode replacement frequency and cost, reducing operational expenditure for challenging industrial effluents. In summary, the synergy of high capacity, selectivity, and long-term stability positions these next-generation CDI electrode materials as promising candidates for scalable deployment, bridging the gap between laboratory performance and practical, economical water treatment.

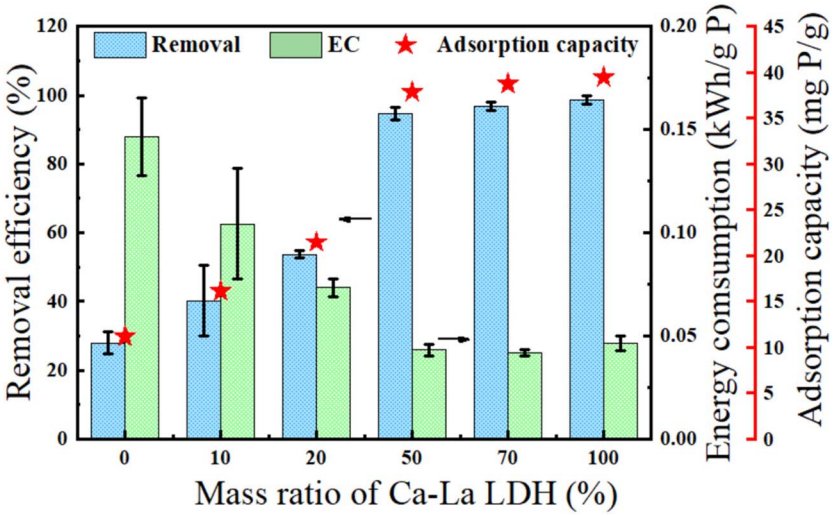

Fig. 9 Effect of Ca–La LDH mass ratio on Cl^- removal efficiency, adsorption capacity, and energy consumption by using CDI technology (reprinted with permission from Desalination,[99] copyright 2024, Elsevier).

4.2. Removal of other anions

4.2.1. CDI technology for sulfate (SO_4^{2-}) removal. SO_4^{2-} is a common high-valence anion in water, primarily originating from mine wastewater, textile dyeing processes, and chemical production. Excessive sulfate concentrations induce both environmental and industrial hazards. Agriculturally, irrigation with high-sulfate water triggers soil salinization and impairs soil aggregate structure.[201] Industrially, sulfate ions react with

Fig. 10 Future development roadmap of CDI applications for anion removal in water treatment and purification.

Ca^{2+} to form $CaSO_4$ scaling, which clogs pipelines and membranes while increasing equipment maintenance costs.[202] Additionally, SO_4^{2-} concentrations exceeding 250 mg L^{-1} in water elevate eutrophication risks.[203] CDI research targeting sulfate removal centers on the development of high-capacity, anti-interference electrodes and configuration optimization, with key advances including: the dual-active biochar CA-NPSSC-1 constructs multi-channel structures through $(NH_4)_2HPO_4$–CO_2 dual activation, achieving a SO_4^{2-} adsorption capacity of 17.16 mg g^{-1} (5.2 times that of unactivated biochar) and an 83.09% removal efficiency in mine wastewater containing Cl^- and NO_3^-.

4.2.2. CDI technology for arsenate (AsO_4^{3-}) removal. AsO_4^{3-}, a highly toxic anion from natural groundwater enrichment, metallurgical wastewater and semiconductor manufacturing, is highly carcinogenic to humans the WHO limits total arsenic in drinking water to <10 μg L^{-1} and long-term exposure leads to skin/lung cancer and nervous system damage.[204] CDI technology is a research focus for ultra-deep arsenate removal with core advances in high-selectivity electrodes and oxidation-adsorption synergy: binder-free electrophoretic-deposited CNTs-X@Fe_3O_4 electrodes use Fe_3O_4 for specific AsO_4^{3-} complexation, oxidize trace As^{3+} to AsO_4^{3-} at 1.2 V (oxidation-adsorption synergy),[205] reducing groundwater arsenic from 0.1 mg L^{-1} to <2 μg L^{-1} and retaining >85% removal with PO_4^{3-} interference. Besides, the Fe-rGO@AC electrodes achieve 49.5 mg g^{-1} AsO_4^{3-} capacity *via* $Fe^0/Fe^{2+}/Fe^{3+}$ cycling, with Fe leaching <0.6 μg L^{-1} after 20 cycles MOF-derived Fe–N–C electrodes maintain >90% removal at pH 6∼10 *via* FeN_x-AsO_4^{3-} coordination, suiting complex water scenarios.

4.2.3. CDI technology for nitrogen oxyanions (NO_3^-/NO_2^-) removal. Nitrogen-oxygen anions (mainly NO_3^-, NO_2^-) are typical water nutrient pollutants: NO_3^- comes from agricultural non-point sources, domestic and industrial sewage, NO_2^- from NO_3^- reduction and industrial nitrification. Excessive concentrations of nitrogen-oxygen anions pose significant health and ecological hazards, NO_3^- concentrations exceeding 50 mg L^{-1} in drinking water induce infantile methemoglobinemia, while NO_2^- forms carcinogenic nitrosamines through reactions with amines; total nitrogen-oxygen anion concentrations above 0.3 mg L^{-1} further aggravate eutrophication and algal blooms. CDI research on these anions focuses on selectivity and reduction-desorption efficiency. Cu/Zn-MOF-derived N-doped porous carbon electrodes reach 42 mg g^{-1} NO_3^- capacity *via* reversible Cu^0/Cu^{2+} redox, with selectivity factor 3.2 in Cl^-/SO_4^{2-}-containing water. Bi-modified carbon electrodes show specific NO_2^- capture, achieving 95% removal *via* Bi–O–N bonding (post-treatment concentration <0.1 mg L^{-1}).[206]

4.3. Selectivity for various anions

Achieving high selectivity for target anions in complex aqueous matrices is a pinnacle challenge in advancing CDI for practical water treatment. Selectivity in CDI is a multifaceted outcome governed by the interplay between the physicochemical properties of the target ion and the engineered characteristics of the electrode material and CDI configuration.[18] Mechanistically, selectivity originates from the precise matching of ion attributes with complementary functionalities in the electrode. For small and hard Lewis base anions like F^- and AsO_4^{3-}, ultra-high affinity is achieved through strong inner-sphere complexation with hard Lewis acid metal centers,[207] especially La^{3+}, Zr^{4+}, and Fe^{3+}, forming thermodynamically favorable and kinetically stable bonds that override competition from background ions like Cl^-. The removal of high-concentration and high-mobility ions like Cl^- in saline environments relies on engineered specificity through reversible redox chemistry, exemplified by Ag^+/AgCl, couple, or through steric and charge-based sieving within tailored porous architectures. For polyvalent oxyanions such as PO_4^{3-} and SO_4^{2-}, selectivity hinges on electronic and steric differentiation.[208] This can be achieved *via* specific ligand exchange, where the anion's geometry and charge density complement the coordination sphere of a metal site, or through preferential electrostatic interactions in charged or confined nanostructures.

To enhance selectivity, several innovative material design strategies have been developed. These include molecular imprinting and covalent grafting to create tailored cavities or functional groups that geometrically and chemically complement the target anion, as well as the use of redox-active sites with inherent specificity, such as metal redox couples that react preferentially with a particular ion.[209] Additionally, designing hybrid and hierarchical structures that combine materials offering distinct selective mechanisms, such as ion exchange, specific complexation, and physisorption, enables a synergistic response to complex ion mixtures.[210] Beyond material design, CDI configuration and operational parameters serve as critical levers for tuning selectivity. MCDI enhances selectivity by incorporating the intrinsic selectivity of IEMs into the electrochemical process. HCDI allows one electrode to be optimized for selective capture *via* faradaic processes while the other manages charge balance. Furthermore, adjusting operational parameters, such as applied voltage and solution pH, can shift the dominant removal mechanism or alter the speciation and affinity of target ions, thereby offering dynamic control over selectivity in practical applications.[121]

5. Conclusions and perspectives

CDI technology for anion removal has advanced significantly but faces bottlenecks in fundamental understanding, materials, and scaling. Key gaps include unclear competitive adsorption dynamics, limited predictive models, and poor system predictability for real waters. Scalability challenges involve high material costs, complex synthesis, module integration issues, and insufficient long-term stability validation. The research paradigm remains lab- and batch-oriented, lacking continuous systems and industry standards. Future work should focus on: (1) fundamental mechanisms for predictive design, (2) cost-effective scalable materials, (3) modular fault-tolerant systems, (4) long-term pilot studies with real water. Early techno-economic and life-cycle analyses are essential. The envisioned roadmap for CDI technology is centered on three key pillars

(Fig. 10), material multifunctionality, system intelligence, and application diversification. Core priorities include the development of cost-effective and high-performance composite electrodes through scalable synthesis, along with the implementation of AI-driven intelligent control and modular system designs. The application scope extends to high-value industrial wastewater from sectors such as semiconductors and textiles, as well as specialized wastewater treatment. By deeply integrating with renewable energy sources like solar and wind, the CDI technology aims to achieve off-grid and carbon-neutral operation, thereby supporting the sustainable goals of the water-energy nexus. Priorities are multifunctional composite electrodes, green scalable synthesis, intelligent real-time control, and compact modular designs. Applications span semiconductor, textile, and agricultural sectors, plus nuclear wastewater and high-salinity brines. Integration with renewable energy (solar, wind) enables off-grid, carbon-neutral operation, supporting water-energy nexus goals and sustainable infrastructure.

The real-world application of CDI technology for water security hinges on overcoming several major challenges to large-scale deployment. First, economic viability remains a primary barrier, driven by the high cost of advanced CDI electrode materials and complex module manufacturing. Second, engineering and system integration must address issues related to scaling up, including maintaining performance uniformity across large electrode stacks, ensuring stable hydraulic flow, and guaranteeing long-term durability of membranes and electrodes under fluctuating real-water conditions. Third, the field currently lacks predictability and standardization, with no universally accepted performance evaluation protocols or predictive models for CDI lifespan under industrial operating conditions. Future solutions must adopt a holistic approach. Economically, research should focus on scalable and cost-effective synthesis routes for electrode materials and the use of earth-abundant alternatives. From an engineering perspective, modular and fault-tolerant architectures that simplify maintenance and enable incremental scale-up are needed. Crucially, long-duration pilot studies using authentic wastewater streams are indispensable to generate robust data for reliable techno-economic and life-cycle assessments. Furthermore, AI offers a transformative toolkit to address these bottlenecks. In electrode design, machine learning accelerates material screening by predicting properties from descriptors. For system optimization, AI algorithms dynamically adjust operating parameters using real-time sensor data to maximize efficiency under fluctuating feedwater quality. Most profoundly, AI provides mechanistic insights by uncovering non-linear patterns in multi-dimensional datasets, revealing structure–activity relationships and competitive adsorption behaviors beyond conventional analysis. Integrating AI, from materials discovery to smart process control, is a pivotal direction for intelligent, cost-effective and large-scale CDI systems.

Bridging the gap from laboratory CDI prototypes to large-scale water treatment demands a coordinated strategy that integrates technical validation, engineering innovation, and economic assessment. This pathway must prioritize long-term pilot studies using real wastewater to evaluate fouling, stability, and operational costs under realistic conditions. Ultimately, advancing CDI for anionic pollutant removal will rely on deep collaboration across material design, system engineering, and application validation to establish performance standards and demonstrate technology readiness in targeted applications.

Author contributions

Yuting Shi: conceptualization, formal analysis, writing–original draft. Haoran Xu: visualization, validation. Jintian Jiang: formal analysis, project administration. Guoqing Xu: methodology, validation. Zhiyang Yu: validation, conceptualization. Wei Zhang: project administration. Shi Jia: methodology, formal analysis, writing–review & editing. Ao Yu: conceptualization, supervision, writing–review & editing. Minjie Shi: resources, funding acquisition, writing–review & editing.

Conflicts of interest

The authors declare that they have no known competing financial interests or personal relationships that could have appeared to influence the work reported in this paper.

Data availability

No primary research results, software or code have been included and no new data were generated or analysed as part of this review. All discussed findings are based on previously published studies cited throughout the manuscript.

Acknowledgements

This work was financially supported by the Funded by Basic Research Program of Jiangsu (No. BK20251919), the Science and Technology Planning Social Development Project of Zhenjiang City (SJC20240100056, JC2024018), and Ministry of Education, under the Academic Research Fund, Singapore (RG88/23).

References

1 V. M. Santhi, D. Periasamy, M. Perumal, P. M. Sekar, V. Varatharajan, D. Aravind, K. Senthilkumar, S. Kumaran, S. Ali, S. Sankar, N. Vijayakumar, C. Boominathan and R. S. Krishnan, *Sustainability*, 2024, **16**, 11056.
2 M. E. Batouti, N. Al-Harby and M. Elewa, *Water*, 2021, **13**, 3241.
3 N. Qasem, R. Mohammed and D. Lawal, *npj Clean Water*, 2021, **4**, 1–15.
4 J. Ayach, W. E. Malti, L. Duma, J. Lalevée, M. A. Ajami, H. Hamad and A. Hijazi, *Polymers*, 2024, **16**, 1959.
5 K. H. Aziz, F. Mustafa, K. Omer, S. Hama, R. Hamarawf and K. Rahman, *RSC Adv.*, 2023, **13**, 17595–17610.

6 G. Singh, G. Yadav, N. Yadav, S. Kapoor, B. Sharma, R. Sharma, R. Kumar and G. Chaudhary, *Adv. Colloid Interface Sci.*, 2024, **336**, 103376.
7 M. Lu, L. Sun, D. Yang, Z. Nie and W. Gong, *Molecules*, 2025, **30**, 1123.
8 A. Periyasamy, *Sustainability*, 2024, **16**, 495.
9 N. Saha, *Sci. Cult.*, 2023, **89**, 21–26.
10 N. Jangid, S. Kaliraman, A. Singh, A. Srivastava, M. Srivastava, S. Jadoun, J. Dwivedi and N. Kaur, *J. Mol. Liq.*, 2024, **399**, 124473.
11 R. Kadhim, B. Khudhair and M. Jaafar, *J. Eng.*, 2023, **29**, 61–77.
12 D. Kovtun and S. Dushkin, *Technog. Ecol. Saf.*, 2023, **2**, 9.
13 X. Huang, S. Guida, B. Jefferson and A. Soares, *npj Clean Water*, 2020, **3**, 1–10.
14 D. Golubenko, R. Al-Juboori, A. Manin, D. Petukhov, A. Yaroslavtsev, D. Johnson and N. Hilal, *Water Res.*, 2025, **283**, 123869.
15 S. Khan, M. Jain, A. Pandey, K. Pant, Z. Ziora, M. Blaskovich, N. Shetti and T. Aminabhavi, *J. Environ. Manage.*, 2022, **319**, 115675.
16 T. Pang, F. Marken, D. Mattia, J. Shen, D. Zhang and M. Xie, *Desalination*, 2024, **592**, 118140.
17 P. Sivasubramanian, M. Kumar, V. Kirankumar, M. Samuel, C.-D. Dong and J.-H. Chang, *Desalination*, 2023, **559**, 116652.
18 F. Xu, L. Yuan, R. Zhao, B. Qin, F. Zhang, L. Ren, H. Yang and M. Yuan, *Materials*, 2025, **18**, 3767.
19 Z. Song, Y. Chen, N. Ren and X. Duan, *Environ. Funct. Mater.*, 2023, **2**, 290–303.
20 K. Sun, M. Tebyetekerwa, C. Wang, X. Wang, X. Zhang and X. Zhao, *Adv. Funct. Mater.*, 2023, **33**, 2213578.
21 H.-F. Deng, Z. Wang, M. Kim, Y. Yamauchi, S. Eichhorn, M. Titirici and L. Deng, *Nano Energy*, 2023, **117**, 108914.
22 Z. Leong, J. Yao, N. Boon, H. Eral, D. Li, R. Hartkamp and H. Yang, *ACS Nano*, 2024, **18**, 29067–29077.
23 R. Zornitta, L. Ruotolo and L. De Smet, *Sep. Purif. Technol.*, 2022, **290**, 120807.
24 M. Ceron, F. Aydin, S. Hawks, D. Oyarzun, C. Loeb, A. Deinhart, C. Zhan, T. Pham, M. Stadermann and P. Campbell, *ACS Appl. Mater. Interfaces*, 2020, **12**, 42644–42652.
25 Y. Guo, H. Feng, L. Zhang, Y. Wu, C. Lan, J. Tang, J. Wang and L. Tang, *Environ. Sci. Technol.*, 2024, **58**, 5589–5597.
26 X. Liu, D. Rehman, Y. Shu, B. Liu, L. Wang, L. Li, M. Wang, K. Wang, Q. Han, L. Zang, J. Lienhard and Z. Wang, *Chem. Eng. J.*, 2024, **482**, 149097.
27 H. Wang, W. Jiang, P. Nie, B. Hu, Y. Hu, M.-N. Huang and J. Liu, *Electrochim. Acta*, 2022, **429**, 141029.
28 J. Wu, *Chem. Rev.*, 2022, **122**, 10821–10859.
29 T. M. Khoi, J. Kim, N. A. T. Tran, V. P. Huynh, Y.-W. Lee and Y. Cho, *Desalination*, 2024, **578**, 117444.
30 X. Zhang, H. Qiu, Z. Han, L. Ke, M. Narayanasamy, C. Cui, J. Yang, M. Shi and E. H. Ang, *Chem. Sci.*, 2025, **16**, 14976–14987.
31 Y.-J. Lin and C. C. Chen, *AIChE J.*, 2023, **69**, e18018.
32 G. Kothandam, G. Singh, X. Guan, J. Lee, K. Ramadass, S. Joseph, M. Benzigar, A. Karakoti, J. Yi, P. Kumar and A. Vinu, *Adv. Sci.*, 2023, **10**, 2206167.
33 K. Yang, Q. Fan, C. Song, Y. Zhang, Y. Sun, W. Jiang and P. Fu, *Green Energy Resour.*, 2023, **1**, 100030.
34 Q. Wu, M. McDowell and Y. Qi, *J. Am. Chem. Soc.*, 2023, **145**, 2473–2484.
35 X.-P. Wang, K. Liu and J. Wu, *J. Chem. Phys.*, 2021, **154**(12), 124701.
36 P. Juchen, K. Barcelos, K. Oliveira and L. Ruotolo, *Chem. Eng. J.*, 2021, **429**, 132209.
37 O. U. Haq, D. Choi, J.-H. Choi and Y.-S. Lee, *J. Ind. Eng. Chem.*, 2020, **83**, 136–144.
38 P. Ren, B. Wang, J. G. De Andrade Ruthes, M. Torkamanzadeh and V. Presser, *Desalination*, 2024, **592**, 118161.
39 X. Huang, L. Huang, S. R. B. Arulmani, J. Yan, Q. Li, J. Tang, K. Wan, H. Zhang, T. Xiao and M. Shao, *Environ. Res.*, 2021, **204**, 112381.
40 R. Wang, Y. Gu, M. Sun and Y. Sun, *Appl. Sci.*, 2025, **15**, 10454.
41 M. Belaye, A. Taddesse, E. Teju, M. Sánchez-Sánchez and J. Yassin, *ACS Omega*, 2023, **8**, 23860–23869.
42 Q. Li, Y. Zheng, D. Xiao, T. Or, R. Gao, Z. Li, M. Feng, L. Shui, G. Zhou, X. Wang and Z. Chen, *Adv. Sci.*, 2020, **7**, 2000978.
43 F. Gao, X. Li and W. Shi, *ACS Appl. Mater. Interfaces*, 2022, **14**, 31962–31972.
44 S. Kim, S.-P. Hong, H. Joo, C. Lee, Y. E. Sung, J. Yoon and J. S. Kang, *Chemsuschem*, 2025, **18**, e202500267.
45 M. Liang, L. Wang, V. Presser, X. Dai, F. Yu and J. Ma, *Adv. Sci.*, 2020, **7**, 1–9.
46 Q. Li, Q. Mao, M. Li, S. Zhang, G. He and W. Zhang, *Carbohydr. Polym.*, 2020, **234**, 115926.
47 W. Tao, H.-C. Zhong, X.-N. Pan, P. Wang, H.-Y. Wang and L. Huang, *J. Hazard. Mater.*, 2020, **384**, 121373.
48 K. Xie, S. Wang, M.-S. Yuan, H. Zhang, H. Deng, Y. Zhang, J. Wang and Y. Zhuang, *Sep. Purif. Technol.*, 2022, **302**, 122152.
49 P. Wang, W. Zuo, B. Li, S. Wang, M. Xu, W. Zhu, Y. Tian and Y. Zhang, *Chem. Eng. J.*, 2023, **470**, 144079.
50 B. Yang, F. Jiang, Y. Zhao, H. Li, S. Zhang and K. Liu, *Arab. J. Chem.*, 2025, **18**, 106079.
51 F. He, M. Bazant and T. Hatton, *J. Electrochem. Soc.*, 2020, **168**, 53501.
52 Y. Shudo, Y. Sugiyama, T. Tomiyama, D. Parajuli, T. Kawamoto and H. Tanaka, *Chem. Lett.*, 2024, **53**, upae187.
53 S. Kang, Y. Kim, V. Wilke, S. Bae, J. Chmielarz, D. Sanchez, K. Ham, A. Gago, K. Friedrich and J. Lee, *ACS Appl. Mater. Interfaces*, 2024, **16**, 47387–47395.
54 L. Peng, J. Min, A. Bendavid, D. Chu, X. Lu, R. Amal and Z. Han, *ACS Appl. Mater. Interfaces*, 2022, **14**, 40822–40833.
55 M. Al-Azwani, S. Al-Busafi and E.-S. El-Shafey, *Heliyon*, 2025, **11**, e42070.
56 S. Saslow, E. Cordova, N. Escobedo, O. Qafoku, M. Bowden, C. Resch, N. Lahiri, E. Nienhuis, D. Boglaienko,

T. Levitskaia, P. Meyers, J. Hager, H. Emerson, C. Pearce and V. Freedman, *J. Hazard. Mater.*, 2023, **459**, 132165.
57 G. Park, S.-P. Hong, C. Lee, J. Lee and J. Yoon, *J. Colloid Interface Sci.*, 2020, **581**, 396–402.
58 W. Li, C. Cui, Q. Wei, H. Chand, A. Wang, N. Pismenskaya and C. Zhang, *Chem. Eng. J.*, 2024, **484**, 149657.
59 Z. Chen, F. Liu, B. Liao, T. Zhang, F. Chen, J. Wang, C. Liao and S. Xu, *Inorganics*, 2025, **13**, 369.
60 H. Zhang, Q. Wang, J. Zhang, G. Chen, Z. Wang and Z.-C. Wu, *Chem. Eng. J.*, 2022, **439**, 135527.
61 X. Liu, W. Cheng, Y.-Y. Yu, S. Jiang, Y. Xu and E. Zong, *Composites, Part B*, 2022, **237**, 109861.
62 K. Rathinam, R. Atchudan and T. Edison, *J. Environ. Chem. Eng.*, 2021, **9**, 106053.
63 C. Chu, R. Li, Q. Chen, W. Li, J. Li and S. Jiang, *J. Colloid Interface Sci.*, 2025, **703**(Pt 1), 139099.
64 J. Song, Y. Yu, X. Han, W. Yang, W. Pan, S. Jian, G. Duan, S. Jiang and J. Hu, *J. Hazard. Mater.*, 2023, **463**, 132843.
65 R. Liu, J. Song, J. Zhao, Z. Wang, J. Xu, W. Yang and J. Hu, *Chem. Eng. J.*, 2024, **497**, 154780.
66 S. Xing, N. Liu, Q. Li, M. Liang, X. Liu, H. Xie, F. Yu and J. Ma, *Nat. Commun.*, 2024, **15**, 3076.
67 S. Girousi, V. Keramari, I. Paraschi, S. Karastogianni and E. Golia, *Chemosensors*, 2025, **13**, 91.
68 X. Jiang, L. Pei, Q. Liu, Z. Lin, S. Liu, H. Wang and X. Lu, *Small Methods*, 2025, **9**, e01457.
69 Y. Kim, H. Cho, Y. Choi, J. Koo and S. Lee, *Membranes*, 2023, **13**, 316.
70 W. Deng, Y. Chen, Z. Wang, X. Chen, M. Gao, F.-F. Chen, W. Chen and T. Ao, *Water Res.*, 2022, **222**, 118927.
71 R. Uwayid, E. Guyes, A. Shocron, J. Gilron, M. Elimelech and M. Suss, *Water Res.*, 2021, **210**, 117959.
72 B. Maqdasi, E. Alhseinat, J. Rodríguez and K. Al-Ali, *Chem. Eng. J. Adv.*, 2025, **13**, 91.
73 Y. T. Maaroof and K. M. Mahmoud, *Bull. Chem. Soc. Ethiop.*, 2022, **37**, 491–503.
74 D. Liu, B. Wei, C. Zhang and Q. Li, *Sep. Purif. Technol.*, 2024, **360**, 131025.
75 K. Tan, X. Su and T. Hatton, *Adv. Funct. Mater.*, 2020, **30**, 2004635.
76 M. Alkhadra, X. Su, M. Suss, H. Tian, E. Guyes, A. Shocron, K. Conforti, J. De Souza, N. Kim, M. Tedesco, K. Khoiruddin, I. Wenten, J. Santiago, T. Hatton and M. Bazant, *Chem. Rev.*, 2022, **122**, 13547–13635.
77 G. Cai, P. Yan, L. Zhang, H. Zhou and H. L. Jiang, *Chem. Rev.*, 2021, **121**, 12278–12326.
78 K. Dassouki, S. Dasgupta, E. Dumas and N. Steunou, *Chem. Sci.*, 2023, **14**, 12898–12925.
79 T. Sharker, J. Gamaethiralalage, Q. Qu, X. Xiao, J. Dykstra, L. De Smet and J. Muff, *Environ. Sci. Pollut. Res. Int.*, 2024, **31**, 63734–63746.
80 M. Qin, A. Deshmukh, R. Epsztein, S. Patel, O. Owoseni, W. Walker and M. Elimelech, *Desalination*, 2019, **455**, 100–144.
81 Y. Jiang, L. Jin, D. Wei, S. Alhassan, H.-Y. Wang and L. Chai, *Int. J. Environ. Res. Public Health*, 2022, **19**, 10599.
82 S. Porada, L. Zhang and J. Dykstra, *Desalination*, 2020, **488**, 114383.
83 S. Patel, M. Qin, W. Walker and M. Elimelech, *Environ. Sci. Technol.*, 2020, **54**, 3663–3677.
84 M. Liu, Z.-H. Xue, H. Zhang and Y. Li, *Electrochem. Commun.*, 2021, **125**, 106974.
85 J. Yang, H. Zhao, C. Li and X.-W. Li, *Renewable Energy*, 2021, **168**, 353–364.
86 C. Lemoine, Y. Petit, T. Karaman, G. Jahrsengene, A. M. Martinez, A. Benayad and E. Billy, *RSC Adv.*, 2024, **14**, 29174–29183.
87 K. Maheshwari, A. B. Gupta, R. Gupta and M. Agarwal, *J. Clean. Prod.*, 2023, **395**, 136405.
88 H. Rosentreter, M. Walther and A. Lerch, *Membranes*, 2021, **11**, 126.
89 X. Ma, W. Wang, L. Zhang, Q. Wu, S. Lu, D. Aurbach and Y. Xiang, *Desalination*, 2021, **520**, 115336.
90 M. Gao, Z. Wang, W. Xiao, L. Miao, Z. Yang, W. Liang, T. Ao and W. Chen, *Desalination*, 2024, **577**, 117392.
91 H. Kang, Z. Lu, D. Zhang, H. Zhao, D. Yang, Z. Wang and Y. Li, *Sep. Purif. Technol.*, 2024, **353**, 128551.
92 S. Hu, D. Fang, F. Li, Z. Xu, K. Li, P. Zhang and W. Feng, *Desalination*, 2025, **601**, 11860.
93 L. Duan, Q. Yun, G. Jiang, D. Teng, G. Zhou and Y. Cao, *J. Environ. Manage.*, 2024, **353**, 120184.
94 E. Laforce, E. Cornelissen, P. Vermeir and J. De Clercq, *J. Environ. Chem. Eng.*, 2025, **13**, 118890.
95 D. Liu, Y. Li, C. Liu and B. Li, *J. Colloid Interface Sci.*, 2023, **636**, 588–601.
96 B. Li, S. Wen, J. Li, D. He, Y. Luo, X. Zheng and D. Chen, *RSC Adv.*, 2025, **15**, 48–57.
97 J. Xiong, W. Ye, L. Mu, X. Lu and J. Zhu, *Small*, 2024, **20**, 2400288.
98 Y. Ge, Y. Wang, Y. Chen, X. Xu, Z. Liu, Z.-S. Yin, Y. Dai, F. Liu and W. Yang, *Chem. Eng. J.*, 2024, **495**, 153462.
99 C. Feng, X. Pan, X. Lin, Y. Yang, F. Fan, C. Jiang and Y. Mei, *Desalination*, 2024, **594**, 118259.
100 L. Song, J. Nan, B. Liu and F. Wu, *Chemosphere*, 2023, **329**, 138016.
101 Q. Li, W. Luo, X. Cui and J. Shi, *Angew. Chem.*, 2025, **64**, e202500303.
102 K. Prasad, M. Kumar, M. Shkir and J.-H. Chang, *J. Sci.:Adv. Mater. Devices*, 2025, **10**(1), 928.
103 M. Moradi, Y. Vasseghian, A. Khataee, M. Kobya, H. Arabzade and E. Drăgoi, *J. Ind. Eng. Chem.*, 2020, **87**, 18–39.
104 J. Wang, H. Ji, J. Li, Z. Liang, W. Chen, Y.-F. Zhu, G. Ji, R. Shi, G. Zhou and H. M. Cheng, *Nat. Sustain.*, 2024, **7**, 1283–1293.
105 H. Liu, G. Tian, W. Wang, J. Zhang, T. Wu, N. Xinye and Y.-H. Wu, *Chem. Eng. J.*, 2020, **399**, 127622.
106 T. Liu, Y. Chen, Y. Hao, J. Wu, R. Wang, L. Gu, X. Yang, Q. Yang, C. Lian, H. Liu and M. Gong, *Chem*, 2022, **8**, 2700–2714.
107 J. Nordstrand and J. Dutta, *Desalination*, 2020, **497**, 114842.
108 B. Lee, C. Oh, J. An, S. Yeon and H. Oh, *Sustainability*, 2023, **15**, 16809.

109 G. Wang, D. Chen, Z. Yang, S. Liao, R. S. Tamjidur, S. Hu, Q. Wu and W. Zhang, *Desalination*, 2025, **602**, 118640.
110 H. Zhang, T. Pang and M. Xie, *Sep. Purif. Technol.*, 2024, **359**, 130411.
111 V. Singh, G. Ahmed, S. Vedika, P. Kumar, S. Chaturvedi, S. Rai, E. Vamanu and A. Kumar, *Sci. Rep.*, 2024, **14**, 7595.
112 M. Bhatt, K. Gautam, A. Rawat, A. Sagdeo, A. Verma and A. Sinha, *Sci. Rep.*, 2025, **15**, 45196.
113 D. Liu, Z. Huang, M. Li, X. Li, P. Sun and L. Zhou, *Carbohydr. Polym.*, 2020, **230**, 115564.
114 Y. Jiang, S. Alhassan, D. Wei and H.-Y. Wang, *Water*, 2020, **12**, 30330.
115 A. Baskar, N. Bolan, S. Hoang, P. Sooriyakumar, M. Kumar, L. Singh, T. Jasemizad, L. Padhye, G. Singh, A. Vinu, B. Sarkar, M. Kirkham, J. Rinklebe, S. Wang, H. Wang, R. Balasubramanian and K. Siddique, *Sci. Total Environ.*, 2022, **833**, 153555.
116 Renu and T. Sithole, *S. Afr. J. Chem. Eng.*, 2024, **50**, 39–50.
117 X. Yang, L. Liu, Y. Wang, T. Lu, Z. Wang and G. Qiu, *Environ. Pollut.*, 2023, **332**, 121002.
118 S.-Q. Jiang, C. Xu, X.-G. Li, C.-Z. Deng, S. Yan and X. Zhu, *J. Environ. Manage.*, 2024, **358**, 120818.
119 A. Ali, M. Sadia, M. Azeem, M. Ahmad, M. Umar and Z. U. Abbas, *Futuristic Biotechnol.*, 2023, **3**, 12–19.
120 W. Xing, J. Liang, W. Tang, D. He, M. Yan, X. Wang, Y.-L. Luo, N. Tang and M. Huang, *Desalination*, 2020, **482**, 114390.
121 L. Wang and S. Lin, *Environ. Sci. Technol.*, 2019, **53**(10), 5797–5804.
122 K. Sun, C. Wang, M. Tebyetekerwa and X. S. Zhao, *Chem. Eng. J.*, 2022, **446**, 137211.
123 P. Ratajczak, M. Suss, F. Kaasik and F. Béguin, *Energy Storage Mater.*, 2018, **16**, 126–145.
124 E. Avraham, B. Shapira, I. Cohen and D. Aurbach, *Curr. Opin. Electrochem.*, 2022, **36**, 101107.
125 J. Ahn, J. Lee, S. Kim, C. Kim, J. Lee, P. Biesheuvel and J. Yoon, *Desalination*, 2020, **476**, 114216.
126 P.-A. Chen, K.-T. Lee and J.-L. Chang, *Green Energy Fuel Res.*, 2025, **2**, 127–138.
127 W. Wang, Y. Zhang, X. Yang, H. Sun, Y. Wu and L. Shao, *Engineering*, 2022, **25**, 204–213.
128 X. Zhang, Y. Li, Z. Yang, P. Yang, J. Wang, M. Shi, F. Yu and J. Ma, *Sep. Purif. Technol.*, 2022, **297**, 121510.
129 O. Weiland, P. Trinke, B. Bensmann and R. Hanke-Rauschenbach, *J. Electrochem. Soc.*, 2023, **170**, 5054505.
130 M. Rezayani, F. Sharif and H. Makki, *J. Mater. Chem. A*, 2022, **35**(10), 18295–18307.
131 A. Hassanvand, G. Chen, P. Webley and S. Kentish, *Water Res.*, 2018, **131**, 100–109.
132 A. Srivastava, B. Gupta, A. Majumder, A. Gupta and S. Nimbhorkar, *J. Environ. Chem. Eng.*, 2021, **9**, 106177.
133 S. Husien, R. El-Taweel, A. Salim, I. Fahim, L. Said and A. Radwan, *Curr. Res. Green Sustainable Chem.*, 2022, **5**, 100325.
134 H. Rosentreter, C. Scope, T. Oddoy, A. Lerch and J. Meier-Haack, *Desalination*, 2024, **599**, 118412.
135 X. Sun, Y. Yin, H. Chen, L. Zhao, C. Wang and J. Wang, *Bioresour. Technol.*, 2025, **431**, 132588.
136 M. Bahdanchyk, M. Hashempour, Z. T. Sarı and A. Vicenzo, *Electrochim. Acta*, 2025, **519**, 145829.
137 N. Liu, L. Yu, B. Liu, F. Yu, L. Li, Y. Xiao, J. Yang and J. Ma, *Adv. Sci.*, 2022, **10**, 2204041.
138 M. Jaoude, E. Alhseinat, K. Polychronopoulou, G. Bharath, I. Darawsheh, S. Anwer, M. Baker, S. Hinder and F. Banat, *Electrochim. Acta*, 2020, **330**, 135202.
139 H. Dong, C. Shepsko, M. German and A. SenGupta, *J. Environ. Chem. Eng.*, 2020, **8**, 103846.
140 S. Guo, F. Zheng, J. Xu, J. Jiang, Z. Cui, C. Wu, Y. Lin, Q. Sun, Y. Zheng and B. Sa, *RSC Adv.*, 2025, **15**, 14363–14374.
141 G. Folaranmi, M. Bechelany, P. Sistat, M. Cretin and F. Zaviska, *Membranes*, 2020, **10**, 145.
142 C. Zhai, F. Yu and J. Ma, *Desalination*, 2023, **560**, 116701.
143 M. Padligur, P. Westerfeld, J. Linkhorst and M. Wessling, *Chem. Eng. J.*, 2024, **504**, 158374.
144 L. Luo and H. Yu, *Environ. Sci. Technol.*, 2025, **59**, 13054–13062.
145 C. Zhang, J. Ma, L. Wu, J. Sun, L. Wang, T. Li and T. Waite, *Environ. Sci. Technol.*, 2021, **54**, 16134–16142.
146 L. Xu, Y. Mao, Y. Zong and D. Wu, *Water Res.*, 2020, **190**, 116782.
147 M. Mohseni, C. Linnartz, S. Echtermeyer, L. Stüwe and M. Wessling, *J. Water Process Eng.*, 2024, **59**, 104954.
148 C. Zhang, L. Wu, J. Ma, M. Wang and T. Waite, *Water Res.*, 2020, **173**, 115580.
149 S. Dahiya and B. Mishra, *Sep. Purif. Technol.*, 2020, **240**, 116660.
150 S. Hawks, A. Ramachandran, S. Porada, P. Campbell, M. Suss, P. Biesheuvel, J. Santiago and M. Stadermann, *Water Res.*, 2018, **152**, 126–137.
151 R. He, Y. Yu, L. Kong, X. Liu and P. Dong, *Chem. Commun.*, 2023, **59**, 12376–12389.
152 J. Gamaethiralalage, K. Singh, S. Sahin, J. Yoon, M. Elimelech, M. Suss, P. Liang, P. Biesheuvel, R. Zornitta and L. C. P. M. de Smet, *Energy Environ. Sci.*, 2021, **14**, 1095–1120.
153 Y. Zheng, N. A. Khan, X. Ni, K. A. I. Zhang, Y. Shen, N. Huang, X. Y. Kong and L. Ye, *Chem. Commun.*, 2023, **59**, 6314–6334.
154 R. Zhao, O. Satpradit, H. Rijnaarts, P. Biesheuvel and A. van der Wal, *Water Res.*, 2013, **47**, 1941–1952.
155 S. Chen, J. Shang, F.-e. Peng, Z. Song, Y. Zheng, Y. Dai, J. Zhu, F. Guo, X. Fu, K. Chu, X. Cao, Y. Ouyang, I. P. Parkin, Y. Zhou, G. He, T. Liu and W. Zong, *ACS Nano*, 2025, **19**, 31870–31881.
156 Z. Huang, Z. Yang, F. Kang and M. Inagaki, *J. Mater. Chem. A*, 2017, **5**, 470–496.
157 Q. Huang, L. Sheng, T. Wu, L. Huang, J. Yan, M. Li, Z. Chen and H. Zhang, *Desalination*, 2024, **587**, 118197.
158 W. Zhao, L. Guo, M. Ding, Y. Huang and H. Yang, *ACS Appl. Mater. Interfaces*, 2018, **10**, 40540–40548.
159 P. Shen, S. Pan, X. Huang and X. Zhang, *Chemosphere*, 2023, **349**, 140912.

160 A. Andriianova, Y. Biglova and A. Mustafin, *RSC Adv.*, 2020, **10**, 7468–7491.
161 M. Chu, W. Tian, J. Zhao, M. Zou, Z. Lu, D. Zhang and J. Jiang, *Chemosphere*, 2022, **307**, 136024.
162 L. Huo, M. Lv, M. Li, X. Ni, J. Guan, J. Liu, S. Mei, Y. Yang, M. Zhu, Q. Feng, P. Geng, J. Hou, N. Huang, W. Liu, X. Y. Kong, Y. Zheng and L. Ye, *Adv. Mater.*, 2024, **36**, 2312868.
163 X. Song, W. Chen, H. Mou and T. Ao, *Sep. Purif. Technol.*, 2024, **348**, 129370.
164 M. Gao, W. Xiao, L. Miao, H. Kong, Z. Yang, W. Liang, T. Ao and W. Chen, *Sep. Purif. Technol.*, 2024, **343**, 127563.
165 P. Xu, J. Bian, Y. Li, J. Wu, X. Sun and Y. Wang, *Environ. Pollut.*, 2022, **315**, 120208.
166 H. Kabir, A. Gupta and S. Tripathy, *Crit. Rev. Environ. Sci. Technol.*, 2020, **50**, 1116–1193.
167 S. Srivastava and S. Flora, *Curr. Environ. Health Rep.*, 2020, **7**, 140–146.
168 S. Wu, Y. Wang, M. Iqbal, K. Mehmood, Y. Li, Z. Tang and H. Zhang, *Environ. Pollut.*, 2022, **304**, 119241.
169 Y.-A. Park, W. Plehwe, K. Varatharajah, S. Hale, M. Christie and C. Yates, *JBMR Plus*, 2024, **8**, e032.
170 S. Lee, I. Han and J. Korean Soc, *Environ. Eng.*, 2022, **44**, 189–194.
171 Q. Tran and P.-H. Lin, *J. Clean. Prod.*, 2021, **333**, 130125.
172 J. He, Y. Yang, Z. Wu, X. Chao, K. Zhang, L. Kong and J. Liu, *J. Environ. Chem. Eng.*, 2020, **8**, 104516.
173 Y. Wei, L. Wang, H. Li, W. Yan and J. Feng, *Front. Chem.*, 2022, **10**, 900660.
174 Q. Huang, S. Xie, L. Sheng, L. Huang, J. Yan, Z. Chen, M. Li and H. Zhang, *Sep. Purif. Technol.*, 2024, **349**, 130171.
175 F. Yu, X. Zhang, P. Liu, B. Chen and J. Ma, *Small*, 2022, **18**, 2205619.
176 Y.-P. Ku, K. Ehelebe, A. Hutzler, M. Bierling, T. Böhm, A. Zitolo, M. Vorokhta, N. Bibent, F. Speck, D. Seeberger, I. Khalakhan, K. J. J. Mayrhofer, S. Thiele, F. Jaouen and S. Cherevko, *J. Am. Chem. Soc.*, 2022, **144**, 10647–10661.
177 X. Zhao, J. Zhang, Z.-C. Dai, Y. Lei, X. Liu and G. Liu, *J. Environ. Chem. Eng.*, 2022, **10**, 108807.
178 C. Ni, C. Liu, Y. Xie, W. Xie, Z. He and H. Zhong, *Environ. Sci. Pollut. Res.*, 2022, **29**, 82740–82761.
179 N. Parveen, S. Chowdhury and S. Goel, *Environ. Sci. Pollut. Res. Int.*, 2022, **29**, 85742–85760.
180 R. Kishor, D. Purchase, G. Saratale, R. Saratale, L. Ferreira, M. Bilal, R. Chandra and R. Bharagava, *J. Environ. Chem. Eng.*, 2021, **9**, 105012.
181 B. Nikravesh, A. Shomalnasab, A. Nayyer, N. Aghababaei, R. Zarebi and F. Ghanbari, *J. Environ. Chem. Eng.*, 2020, **8**, 104244.
182 P. Xu, Q. Zhang, H. Qian and W. Qu, *Minerals*, 2020, **10**, 199.
183 T. Balasubramaniam, G. Shen, N. Esmaeili and H. Zhang, *Plants*, 2023, **12**, 2253.
184 F. R. A. Z. Rivera, B. P. Pano, S. Guédron, M. Palomino, C. P. De León Hill and C. S. Grabach, *J. Soils Sediments*, 2023, **23**, 2726–2743.
185 F. R. A. Z. Rivera, B. Prado, L. Mora, C. A. P. De León-Hill and C. Siebe, *SSRN Electron. J.*, 2022, DOI: 10.2139/ssrn.4043400.
186 B. Kończak and E. Janson, *J. Water Health*, 2021, **19**(2), 288–305.
187 H. Tamura, M. Kashiura, H. Taira, S. Amagasa and T. Moriya, *Am. J. Emerg. Med.*, 2025, **99**, 515–517.
188 M. Pucci, P. Theodorou and N. Patel, *Clin. Toxicol.*, 2022, **60**, 1292–129.
189 A. Amiri, Y. Chen, C. Teng and M. Naraghi, *Energy Storage Mater.*, 2020, **25**, 731–739.
190 Z. Cao, H. Hu and D. Ho, *Adv. Funct. Mater.*, 2022, **32**, 2205678.
191 C. Zhang, Y.-Z. Qiu, H. Wu, Y.-Q. Jiang, Z.-H. Wan, W.-Q. Fei, Q. Li, W.-W. Li and X.-F. Sun, *Adv. Mater.*, 2025, **38**, e07679.
192 D. Zhang, F. Xie, H. Gong, T. Liu, P. Kuang and J. Yu, *J. Colloid Interface Sci.*, 2023, **658**, 127–136.
193 J. Chang, Y. Li, F. Duan, C. Su, Y. Li and H. Cao, *Sep. Purif. Technol.*, 2020, **240**, 116600.
194 S. Zhao, X. Shi, B. Sun, Y. Liu, Z. Tian and J. Huotari, *Water Sci. Technol.: Water Supply*, 2022, **22**, 1231–1243.
195 L. Kou, J. Zhang, L. Huang, G. Chen, S. Jiang, D. Han and D. Jiang, *Heliyon*, 2025, **11**, e00123.
196 H. Chen, Z. Han, X. Yan, Z. Bai, Q. Li and P. Wu, *J. Environ. Manage.*, 2024, **366**, 121919.
197 W. Feng, T. Wang, Y. Zhu, F. Sun, J. Giesy and F. Wu, *Carbon Res.*, 2023, **2**, 12.
198 J. Chang, F. Duan, C. Su, Y. Li and H. Cao, *Natl. Sci. Rev.*, 2020, **6**, 373–382.
199 X. Song, X. Chen, W. Chen and T. Ao, *J. Electroanal. Chem.*, 2024, **964**, 118312.
200 Y. He, T. Feng, Q. Huang, C. Zhang and G. Li, *Chemosphere*, 2024, **364**, 142973.
201 D. Zak, M. Hupfer, Á. Cabezas, G. Jurasinski, J. Audet, A. Kleeberg, R. McInnes, S. Kristiansen, R. Petersen, H. Liu and T. Goldhammer, *Earth-Sci. Rev.*, 2020, **212**, 103446.
202 Z. Cao, Y. Hu, H. Zhao, B. Cao and P. Zhang, *Water Res.*, 2022, **222**, 118945.
203 M. Chu, W. Tian, J. Zhao, D. Zhang, M. Zou, Z. Lu and J. Jiang, *Desalination*, 2023, **556**, 116588.
204 K. Patel, P. Pandey, P. Martín-Ramos, W. Corns, S. Varol, P. Bhattacharya and Y. ZhuRSC, *Adv.*, 2023, **13**, 8803–8821.
205 L. Cai, B. Xu, Y. Gan, Y. Liu, Z. Chen, W. Yang, J. Zhang and K. Jiang, *Sep. Purif. Technol.*, 2023, **330**, 125419.
206 Y. Liu, Y. Xin, Z.-B. Sun, J.-Q. Wan, Z.-P. Li, Z.-F. Shang, X.-S. Zhang, W.-Z. Li and J. Luan, *Carbon*, 2025, **238**, 216490.
207 M. Tauk, M. Bechelany, P. Sistat, R. Habchi, M. Cretin and F. Zaviska, *Desalination*, 2024, **579**, 117146.
208 L. Pincus, H. Rudel, P. Petrović, S. Gupta, P. Westerhoff, C. Muhich and J. B. Zimmerman, *Environ. Sci. Technol.*, 2020, **54**, 12181–12191.
209 L. Chemeri, B. Nisi, A. Pierozzi, J. Cabassi, M. Taussi, S. Venturi, A. Huertas and O. Vaselli, *J. Environ. Sci.*, 2025, **159**, 250–262.
210 P. Goyal, C. S. Tiwary and S. Misra, *J. Environ. Manage.*, 2020, **277**, 111469.